DIVISION OF STRUCTURES AND ENGINEERING SERVICES

TRANSPORTATION LABORATORY

RESEARCH REPORT

Fatigue Crack Growth In ASTM A-517 Type Steels

FINAL REPORT

CA-DOT-TL-6827-1-76-42

JUNE 1976

76-42

Caltrans

CALIFORNIA DEPARTMENT OF TRANSPORTATION

ClibPDF - www.fastio.com

ClibPDF - www.fastio.com

TECHNICAL REPORT STANDARD TITLE PAGE

1. REPORT NO.	2. GOVERNMENT ACCESSION NO.	3. RECIPIENT'S CATALOG NO.
CA-DOT-TL-6827-1-76-42		

4. TITLE AND SUBTITLE	5. REPORT DATE
FATIGUE CRACK GROWTH IN ASTM A-517 TYPE STEELS	June 1976
	6. PERFORMING ORGANIZATION CODE
7. AUTHOR(S) W. F. Crozier, R. D. Sunbury, C. B. Kendrick, and W. N. Richards	8. PERFORMING ORGANIZATION REPORT NO. 19601-646827
9. PERFORMING ORGANIZATION NAME AND ADDRESS Office of Transportation Laboratory California Department of Transportation Sacramento, California 95819	10. WORK UNIT NO.
	11. CONTRACT OR GRANT NO.
12. SPONSORING AGENCY NAME AND ADDRESS California Department of Transportation Sacramento, California 95807	13. TYPE OF REPORT & PERIOD COVERED Final Report
	14. SPONSORING AGENCY CODE

15. SUPPLEMENTARY NOTES

16. ABSTRACT

The results of a series of fatigue tests on 14 precracked compact tension specimens sampled from three heats of steel plate are presented. Although all three heats generally complied with ASTM Designation: A-517, they possessed a wide range of fracture toughness. The primary objective of the research was to determine if there is merit to a relationship between crack growth rate, fracture toughness and stress ratio in a fatigue environment simulating a cracked girder flange. The cyclic load levels were chosen to represent dead and live load stresses that would be expected in a bridge flange designed with 100 ksi yield strength steel. All tests were performed in air at room temperature.

The report includes graphs of crack length versus number of cycles and crack growth rate versus stress intensity range.

These data indicate that the crack growth rate in ASTM A-517 type steels may be affected by fracture toughness and stress ratio. Since the number of tests was limited, recommendations are made for further research testing and fracture mechanics analyses.

17. KEY WORDS	18. DISTRIBUTION STATEMENT
Fatigue tests, structural steel, toughness, cracking, bridges/ structures, fracture.	No restrictions. This document is available to the public through the National Technical Information Service, Springfield, VA 22161.

19. SECURITY CLASSIF. (OF THIS REPORT)	20. SECURITY CLASSIF. (OF THIS PAGE)	21. NO. OF PAGES	22. PRICE
Unclassified	Unclassified	42	

HMRT – 1242 (ORIG. 9/72)

ClibPDF - www.fastio.com

ClibPDF - www.fastio.com

STATE OF CALIFORNIA
DEPARTMENT OF TRANSPORTATION
DIVISION OF STRUCTURES AND ENGINEERING SERVICES
OFFICE OF TRANSPORTATION LABORATORY

June 1976
TL No. 646827

Mr. C. E. Forbes
Chief Engineer

Dear Sir:

I have approved and now submit for your information this final research project report titled:

FATIGUE CRACK GROWTH
IN ASTM A-517 TYPE STEELS

Study made by .....Structural Materials Branch

Under the Supervision of .....Eric F. Nordlin, P. E.

Principal Investigators .....J. R. Stoker, P. E.
P. G. Jonas, P. E.

Co-Principal Investigators .....W. F. Crozier, P. E.
C. B. Kendrick, P. E.
R. D. Sunbury, P. E.

Principal Assistant .....W. N. Richards, C.E.T.

Report Prepared by .....W. F. Crozier, P. E.

Very truly yours,

George A. Hill

GEORGE A. HILL
Chief, Office of Transportation Laboratory

Attachment
WFC:bjs

ClibPDF - www.fastio.com

ClibPDF - www.fastio.com

ACKNOWLEDGEMENTS

The contents of this report reflect the views of the Office of Transportation Laboratory which is responsible for the facts and the accuracy of the data presented. The contents do not necessarily reflect the official views or policies of the State of California. This report does not constitute a standard, specification, or regulation.

The author wishes to express special appreciation to Carl E. Hartbower of the Federal Highway Administration for his very valuable assistance in an advisory capacity. The author also wishes to extend appreciation for the able assistance provided by Ron Castle, Kerry Wilson, and the Machine Shop staff of the Office of Transportation Laboratory, and Pat McCabe of the Office of Special Projects.

ClibPDF - www.fastio.com

ClibPDF - www.fastio.com

TABLE OF CONTENTS

		Page
	ACKNOWLEDGEMENTS	i
	GLOSSARY	1
I.	INTRODUCTION	2
II.	CONCLUSIONS AND RECOMMENDATIONS	4
III.	TECHNICAL DISCUSSION	5
	A. Material Properties and Preparation of Compact Tension Specimens	5
	B. Test Equipment and Procedures	10
	C. Data Reduction Procedures	13
	D. Test Results and Discussion	15
IV.	REFERENCES	24
V.	APPENDIX	25
	A. Test Results for Each Specimen	25

ClibPDF - www.fastio.com

ClibPDF - www.fastio.com

GLOSSARY

The following descriptions are intended to assist the reader who is unfamiliar with fracture mechanics terminology, and are not necessarily complete definitions of the terms.

Stress, S: The applied load per unit area normally expressed in the units of kips per square inch (ksi).

Stress Range, ΔS: The algebraic difference between the maximum stress and the minimum stress.

Stress Ratio, R: The dimensionless quantity equal to the minimum stress divided by the maximum stress.

Stress Intensity, K: A measure of the stress-field intensity near the tip of a crack in a relatively thick structural member such as a bridge girder flange or suspender bar. The stress intensity is proportional to both the applied stress and the square root of the crack length, and is normally expressed in the units of ksi $inch^{1/2}$. If the stress intensity is allowed to increase until it equals the fracture toughness of the material, the material will fracture.

Stress Intensity Range, ΔK: The algebraic difference between the maximum stress intensity and the minimum stress intensity.

Fracture Toughness, K_{max}: A measure of the resistance of a material to fracture under conditions such as a cracked, relatively thick, bridge girder flange or suspender bar. Historically, the fracture toughness has been considered to be the square root of the product of the energy per unit area required to fracture a specimen, times the Modulus of Elasticity of the material, and is normally expressed in units of ksi $inch^{1/2}$.

ClibPDF - www.fastio.com

I. INTRODUCTION

In connection with the Bryte Bend Bridge litigation, a study was initiated to obtain comparative data on the fatigue life and fatigue crack growth rate of the low toughness casuality flange and two other heats of ASTM A517 type steels with fracture toughness at expected levels. The testing of two specimens had been completed when the case was settled. One specimen was from the Bryte Bend Bridge casuality flange and the other was from the Tuolumne River Bridge replacement flange material. The casualty flange, melted by Lukens Steel Company, was low in fracture toughness and the Tuolumne River Bridge flange plate, melted by U. S. Steel, had a high level of toughness. A dramatic difference in fatigue life and fatigue crack growth rate was exhibited by the two specimens tested. The casualty flange specimen had a fatigue life of only approximately 25% of the Tuolumne River Bridge flange specimen. This finding appeared to be in direct conflict with the current AASHTO design specification which indicates identical fatigue life for all bridge steels regardless of fracture toughness or stress ratio. For example, AASHTO(1) simply specifies an allowable stress range of 12.5 ksi for a welded connection detail such as that used on the casualty flange of the Bryte Bend Bridge.

Recognizing the fact that two tests are not conclusive, this research project was initiated to complete the testing of the remaining twelve (12) wedge opening loading (WOL) specimens, that had been machined and polished, and to report the test results from all fourteen (14) specimens.

The primary objective of this research project was to test one-inch thick WOL (compact tension) specimens from three heats of ASTM A517 type steels, with known differences in fracture toughness, and collect data on the fatigue crack growth rate to determine if there is merit to a relationship between crack growth rate, fracture toughness and stress ratio.

ClibPDF - www.fastio.com

Secondly an evaluation of the data was used in developing recommendations for additional research on a broader scale to include other bridge steels and various stress levels with appropriate stress ratios.

A literature search was conducted, as a part of the Bryte Bend litigation preparation, which produced approximately 30 papers, articles and reports on fatigue crack growth rate. A small amount of these consider the effect of toughness and stress ratio. References 2 through 6 are most pertinent to this report.

ClibPDF - www.fastio.com

II. CONCLUSIONS AND RECOMMENDATIONS

ASTM A517 steels possessing relatively low levels of toughness, say 60 ksi inch$^{1/2}$, exhibit substantially higher crack growth rates than similar steels with levels of toughness of, say, 150 ksi inch$^{1/2}$, at stress levels simulating those in a bridge girder flange. Further research testing is needed to quantify the relationship between crack growth rate and fracture toughness - especially at toughness levels intermediate to the above.

Although the crack growth rate is primarily dependent upon stress intensity range, these data also indicate that the crack growth rate may be significantly affected by stress ratio in ASTM A-517 steels possessing the higher levels of toughness. Further research testing is needed to quantify this relationship at stress ratios normally encountered in bridge structures.

Further research testing is needed to verify the analytical relationship between the fatigue behavior of laboratory test specimens (such as compact tension specimens) and the fatigue behavior of actual structural members (such as bridge girder flanges).

ClibPDF - www.fastio.com

III. TECHNICAL DISCUSSION

A. Material Properties and Preparation of Compact Tension Specimens

A total of fourteen (14) one-inch WOL (compact tension) specimens were machined from three heats of steel produced by different manufacturers. Six "Q" specimens were from the Bryte Bend Bridge 2 1/4 inch thick casualty flanges, melted by Lukens Steel Company, and were modified ASTM A517 grade H steel. Four "D" specimens were from the Tuolumne River Bridge 2 1/2 inch thick flange replacement plate, melted by U. S. Steel, and were ASTM A517 grade F steel. Four "CL" specimens were from a 2 inch thick Caltrans Laboratory research plate, melted by Armco Steel Corp. This plate was melted prior to the existance of the ASTM A517 and was known as a Sheffield Super Strength 100 steel.

A review of mill test reports and supplementary tests performed by the Caltrans laboratory indicated that representative material properties at the quarter point of the thickness of the plates were as shown in Figure 1. The longitudinal direction is defined as the direction of final rolling. Of primary interest in this study was the substantial difference in fracture toughness of the CL and D heats as opposed to the Q heat. The toughness values of Figure 1 were based upon the results of the crack growth rate tests as described in Section III. A series of static compact tension tests performed in accordance with ASTM E399 at 70°F indicated that the toughness of the Q heat in the longitudinal direction was 57 ksi inch$^{1/2}$ - about 10% less than the value shown in Figure 1. This would indicate that all the toughness values shown in Figure 1 may be slightly higher than ASTM E399 toughness values.

ClibPDF - www.fastio.com

FIGURE 1

SUMMARY OF MATERIAL PROPERTIES

Heat	CL		D		Q	
Plate Thickness, in.	2		2 1/2		2 1/4	
Orientation	Trans	Long	Trans	Long	Trans	Long
Tensile Strength, ksi	128	132	120		135	135
Yield Strength, ksi	116	119	109		126	126
Elongation, % in 2"	18	19	19		15	15
Reduction of area, %	61	65	56		44	45
Bend, 180°, D = 3T		Pass	Pass		Pass	Pass
CVN Charpy, 70°F, ft-lbs	25	63	43	61	7	7
PCI Charpy, 70°F, ft-lbs	17	43	30	40	5	5
Toughness*, 70°F, ksi-in.$^{1/2}$		134		138		63
Carbon, %	.17		.14		.22	
Manganese, %	.59		.91		1.11	
Phosphorus, %	.015		.015		.015	
Sulfur, %	.028		.019		.020	
Silicon, %	.32		.23		.30	
Nickel, %			.83		.34	
Chromium, %	1.65		.44		.47	
Molybdenum, %	.51		.46		.30	
Boron, %					.005	
Vanadium, %			.031		.065	
Titanium, %	.05		.005		.04	
Zirconium, %			0			
Copper, %	.28		.22		.22	
Aluminum, %	.05		Tr.			

*Average values from crack growth rate tests described in Section III of this report.

Note: Blank spaces indicate that no tests were performed. Tensile and bend tests were not performed on Heat D in the longitudinal orientation because there was not enough material available.

ClibPDF - www.fastio.com

A total of 14 compact tension specimens were machined as shown in Figure 2 - six from the Q heat and four each from the D heat and CL heat. All the specimens were taken from the plates such that the center of the specimen corresponded to a quarter point through the thickness of the plate, and all were oriented such that the crack would be propagated perpendicular to the final rolling direction. The basic specimen dimensions corresponded to those used in similar research testing by U. S. Steel(2) and Westinghouse(6). In addition, the mouth of each specimen was machined as shown in Figure 2 to receive a clip gage for data acquisition purposes.

Following machining, each specimen was polished on the surfaces where the crack would propagate so that the crack would not be confused with surface scratches. After polishing, a line of indentations as shown in Figure 2 were made at 0.010 inch (0.25 mm) intervals using a Kentron Microhardness Tester. The line of indentations started at a = 1.0 inches and ran parallel to the anticipated crack about 1/16 inch from the crack such that the indentations would not affect the crack growth. These indentations were used to monitor crack growth as described in Section III.C.

Prior to loading, the specimens were bathed in alcohol to remove any moisture or oil which might affect the test results.

The specimens were precracked using the same testing machine and fixtures described in Section III.B. With the exception of specimens Q-5 and Q-6, all specimens were precracked through fatigue loading until the crack length, a, was approximately one inch as shown in Figure 2. Specimens Q-5 and Q-6 were precracked until the crack length, a, was approximately 0.95 inches. For all specimens the maximum precrack load level was kept below the maximum load level of the test so as to minimize the possibility of the precrack loading affecting the test results. The precrack loadings were as follows:

ClibPDF - www.fastio.com

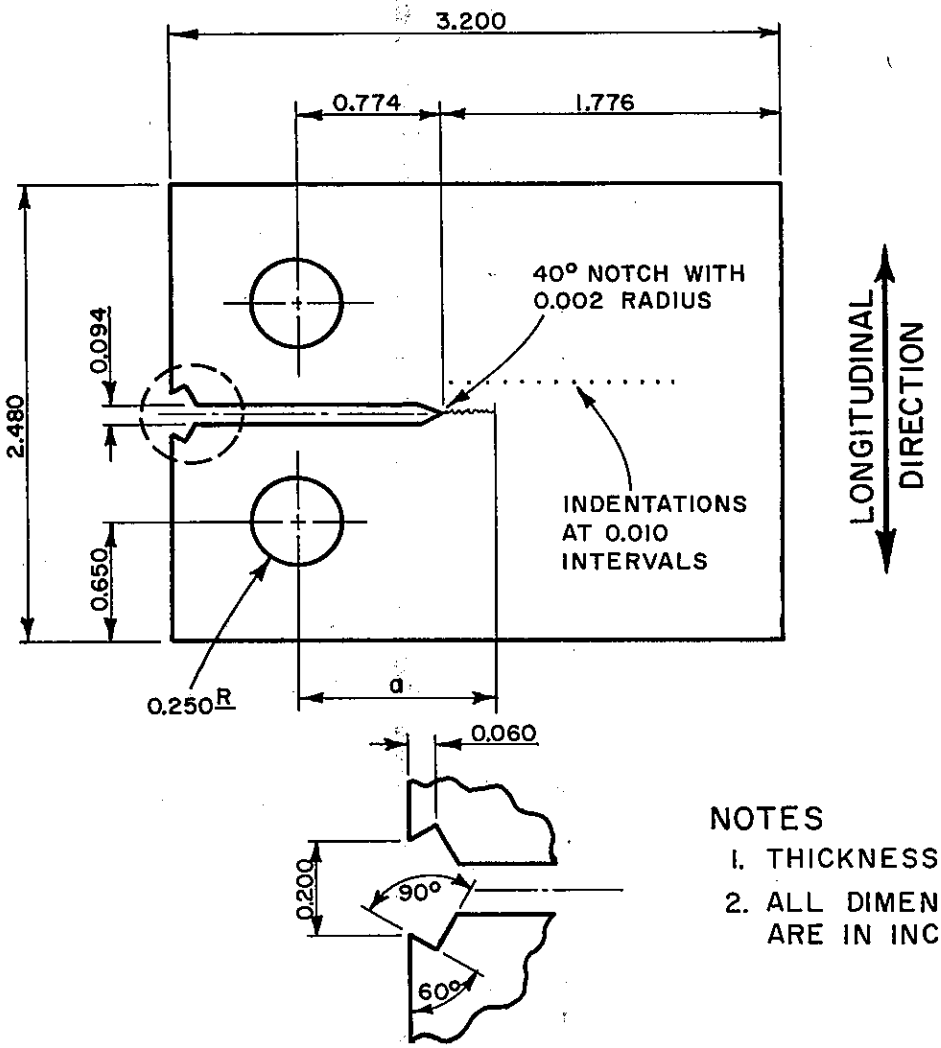

DETAIL

NOTES

1. THICKNESS = 1.000"
2. ALL DIMENSIONS SHOWN ARE IN INCHES

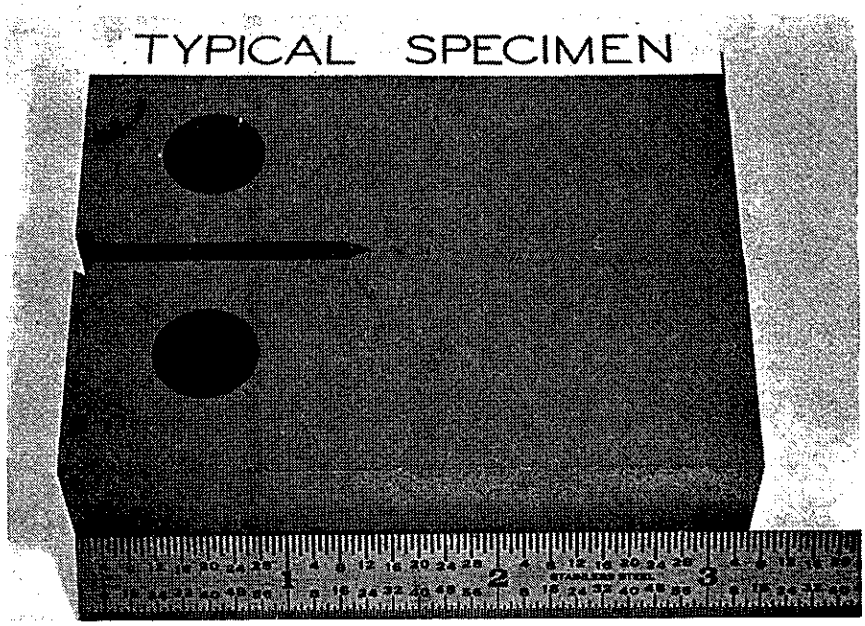

COMPACT TENSION SPECIMEN

FIGURE 2

ClibPDF - www.fastio.com

Specimen	Frequency, cpm	Min. Load, lbs	Max. Load, lbs	No. of Cycles, Cumulative
CL-1	600	800	8000	29,100
	600	2000	8000	33,200
	300	4000	8000	38,500
	300	6000	8000	83,100
CL-2	600	800	8000	34,400
	300	800	8000	35,800
CL-3	600	600	6000	80,300
CL-4	600	600	6000	71,100
D-1	600	800	8000	31,400
	600	2000	8000	35,300
	300	4000	8000	44,800
	300	6000	8000	57,700
D-2	600	800	8000	30,300
	300	800	8000	31,100
D-3	600	800	8000	30,700
D-4	600	800	8000	29,700
	300	800	8000	30,000
Q-1	600	800	8000	21,200
	600	2000	8000	22,800
	300	4000	8000	32,100
	300	6000	8000	52,800
Q-2	600	800	8000	28,500
Q-3	600	600	6000	58,900
Q-4	600	600	6000	55,400
	300	600	6000	56,000
Q-5	600	1000	10,000	12,000
Q-6	600	1000	10,000	12,100

ClibPDF - www.fastio.com

In many cases the rate of precracking was reduced (by decreasing the frequency or stress range) as the precrack approached the desired length in order to avoid "overshooting" the desired precrack length, a. A review of the fatigue test data did not indicate that the variations in the precrack loadings presented above had any apparent effect on the behavior of the specimens during the fatigue tests.

B. Test Equipment and Procedures

The test procedure used was generally the same as that in the NCHRP 12-14 Study(2). The primary difference in the procedure was the starting stress and the stress ratio. The NCHRP 12-14 tests were conducted at a 10 percent stress ratio (R = .10), while this project used stress ratios of 0.78, 0.73 and 0.66 corresponding to maximum starting stresses of 55 ksi, 45 ksi and 35 ksi respectively. These represent stresses that would be expected in a bridge design with 100 ksi yield strength steel.

The original proposal was to test two specimens each of Q, D and CL with a maximum working stress of 45 ksi, followed by two each at 35 ksi, and the two remaining Q specimens at 55 ksi. The proposal was altered when specimen D-2 gave a somewhat shorter fatigue life than D-1. The decision was then made to test all four D specimens at a maximum starting stress of 45 ksi in order to increase confidence in the data at this stress level.

The tests were performed on a Series 810 MTS Test System, shown in Figure 3, which was equipped with a 75 kip capacity actuator. For all tests the loads were applied sinusoidally in tension at 300 cycles per minute between constant minimum and maximum loads. The loads were recorded on a Brush Oscillograph at regular intervals to verify their accuracy. All tests were performed in air at room temperature.

ClibPDF - www.fastio.com

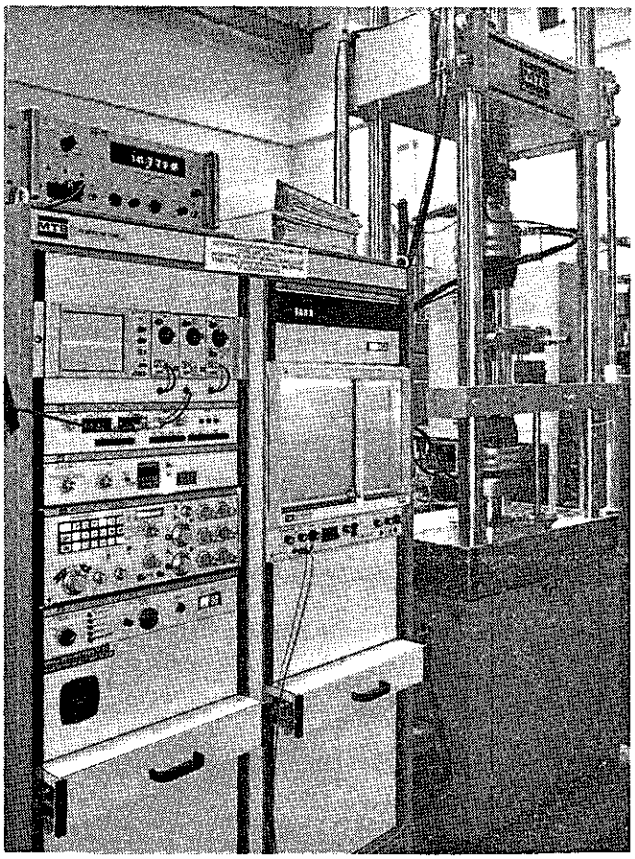

FIGURE 3, 810 MTS SYSTEM WITH TEST IN PROGRESS

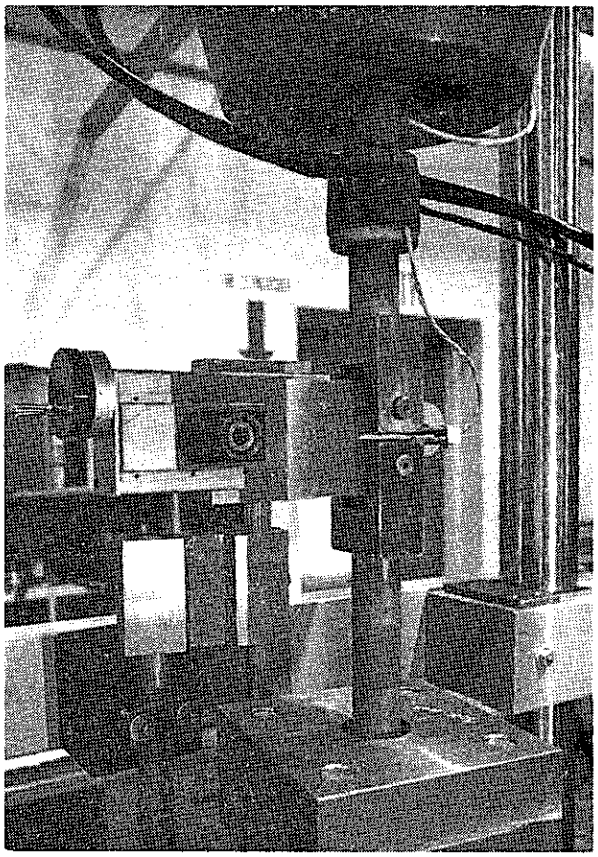

FIGURE 4, TYPICAL TEST SET-UP

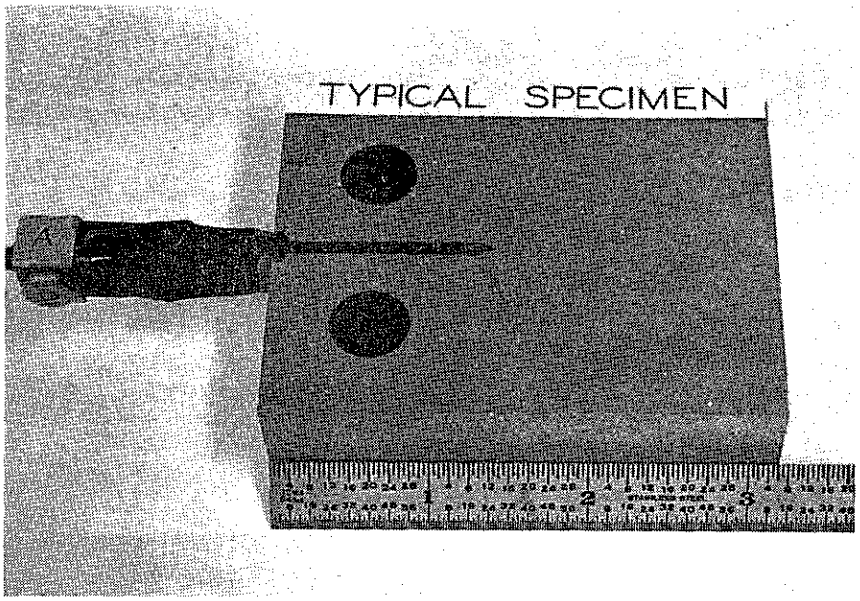

FIGURE 5, CLIP GAGE IN PLACE

ClibPDF - www.fastio.com

Three separate methods were used to monitor the crack length:

1. A traveling micrometer microscope was mounted on the loading frame of the testing machine as shown in Figure 4. Using a 17X lens and a vernier reading to the nearest 0.01 millimeter, the crack length was recorded at maximum intervals of 0.02 inch (with a few exceptions) throughout the tests. This crack length data, along with the cumulative cycle count from the testing machine, provided the bases for all the crack growth data presented in this report.

2. The indentations on each specimen, described in Section III.A., were placed on the same side of the specimen as the microscope. By visually interpolating between the indentations, crack length data was obtained which served as a rough check of the data obtained in 1. above.

3. A clip gage was placed in the mouth of each specimen as shown in Figure 5 to measure the crack opening displacement (COD). The COD's were recorded on dual ranged galvanometers of the Brush Oscillograph each time microscope readings were recorded. Because analysis of this data did not fall within the scope of this research project, the data is not presented in this report, but it is hoped that it will serve as valuable raw data in future research.

In general, the crack length and corresponding number of cycles were recorded at intervals not exceeding 0.02 inch. Because the testing was limited to regular working hours, many of the tests were interrupted at the end of each eight hour shift. In these cases the specimens were removed from the testing machine until the next test day. Before resuming a test, the clip gage was again calibrated and new crack length readings were recorded. Because the position of the test specimen and/or microscope might vary slightly as a result of the interruption, the crack

ClibPDF - www.fastio.com

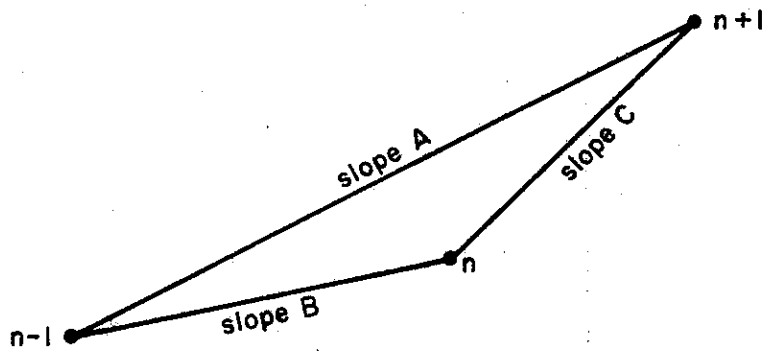

$$\text{Slope @ } n = \frac{2\,(\text{slope A}) + \text{slope B} + \text{slope C}}{4}$$

DEFINITION OF SLOPE (da/dN) AT EACH DATA POINT

FIGURE 6

ClibPDF - www.fastio.com

length data reduction process included correction factors to reconcile any differences between readings taken before and after the interruption. A review of all test data following the tests indicated that such interruptions had no apparent effect upon crack growth rate.

C. Data Reduction Procedures

Selected "a" (crack length) versus "N" (number of cycles) data was fed to a digital computer program in order to establish the crack growth rate which is normally expressed in terms of "da/dN" as a function of "ΔK"(2,6).

ClibPDF - www.fastio.com

For each data point, the crack growth rate, "da/dN", was calculated as defined in Figure 6. Also calculated was the stress intensity range, "ΔK", which was defined as(2):

$$\Delta K = \frac{C_3 \ (\Delta P)}{B \sqrt{a}} \qquad (1)$$

Where:

ΔK = stress intensity range, ksi $inch^{1/2}$
ΔP = range of applied load, kips
B = specimen thickness, inches
a = crack length measured from loading plane, inches
$C_3 = 30.96\ (a/w) - 195.8\ (a/w)^2 + 730.6\ (a/w)^3 - 1186.3\ (a/w)^4 + 754.6\ (a/w)^5$
W = horizontal distance from loading plane to the far end of the specimen, inches

With this data, the program then established the "best fit" for the equation:

$$da/dN = c(\Delta K)^m, \qquad (2)$$

which is known as the Paris equation, where the constants "c" and "m" are determined by the program. Equations of this form are commonly used to analytically predict the fatigue life of cracked structural members, and appear as straight lines on log-log graphs of "da/dN" versus "ΔK". This linear portion of the crack growth rate curve is known as the region of sub-critical crack growth or Region II. As the crack grows, a certain threshhold point is reached where the crack grows very rapidly and non-linearly in what is known as Region III. In order to restrict equation (2) to the linear portion (Region II) of the crack growth rate curves, the "a" versus "N" data which was obviously non-linear (Region III) was withheld from the computer program.

ClibPDF - www.fastio.com

Equation (1) was also used to estimate the fracture toughness of the material in each test specimen. After failure, the toughness was calculated based upon the maximum load and final crack length as measured from the fracture face in accordance with ASTM E399, i.e., the average of three measurements taken at the quarter-points and at the center point. Because of the nature of the fracture of the Q specimens, the final crack length was difficult to measure from these specimens.

D. Test Results and Discussion

The initial test conditions and test results are summarized in Figure 7. Detailed test data and photographs of each specimen are presented in the Appendix.

The applied load ranges were chosen such that the tensile stresses at the crack tip would simulate those in an ASTM A517 girder flange when the crack length, "a", was equal to one inch. At this crack length, the live load stress range was 12 ksi for all tests. Stresses at the crack tip of the one inch wide specimens were calculated from the equation:

$$S = \frac{P}{(W-a)^2} \quad (4\ W + 2a)$$

Where: S = stress, ksi
P = applied load, kips
a = crack length measured from loading plane, inches
W = horizontal distance from loading plane to the far end of the specimen, inches.

Figure 8 illustrates the effect of variations in toughness upon specimen behavior. The specimen fatigue life of the Q-2 specimen, which possessed about 40% of the toughness of the D-2 and CL-2 specimens, was about 40% of the specimen fatigue life of the D-2

ClibPDF - www.fastio.com

FIGURE 7

SUMMARY OF TEST RESULTS

Specimen	Pmin[1]/Pmax kips	R	Initial Smin[2]/Smax ksi	Initial a in.	At Failure a[3] in.	At Failure Kmax[3] ksi√in.	At Failure N x10^3	Rate da/dN=C (ΔK)^M C x10^exp	Rate M
CL-1	6.50/8.86	0.73	33/45	1.025	1.854	141	435.3	.251 -9	3.15
CL-2	"	"	"	1.029	1.831	134	450.7	.656 -10	3.64
D-1	"	"	"	1.026	1.862	143	607.6	.105 -10	4.20
D-2	"	"	"	1.024	1.843	137	374.0	.251 -9	3.22
D-3	"	"	"	1.027	1.827	133	346.9	.353 -9	3.11
D-4	"	"	"	1.038	1.844	138	331.9	.160 -9	3.40
Q-1	"	"	"	1.024	1.34	61	166.9	.266 -12	6.03
Q-2	"	"	"	1.045	1.36	63	163.7	.323 -15	8.62
CL-3	4.53/6.89	0.66	23/35	1.027	1.929	130	419.4	.758 -9	2.76
CL-4	"	"	"	1.032	1.933	131	444.9	.476 -9	2.93
Q-3	"	"	"	1.030	1.51	59	253.6	.239 -9	3.31
Q-4	"	"	"	1.028	1.58	65	264.2	.853 -10	3.70
Q-5	8.47/10.83	0.78	43/55	0.951	1.13	61	115.3	- -	- -
Q-6	"	"	"	0.957	1.30	72	85.6	.735 -10	17.1

1. For all tests the load, P, was applied sinusoidally at 300 cpm with the minimum and maximum loads held constant throughout each test.

2. Smin and Smax are the nominal stresses at the crack tip when crack length, "a", is one inch.

3. "a" and "K" at failure were based upon measurements of the fracture face as described in Section III.c.

ClibPDF - www.fastio.com

and CL-2 specimens. The crack length of the Q-2 specimen at failure was also much shorter because of the lower toughness. Figure 9 illustrates the difference in the fracture faces due to variations in toughness. While the Q-2 specimen exhibited a very flat fracture face with little lateral reduction, the CL-2 and D-2 specimens exhibited more ductile behavior. The substantially higher crack growth rate of the Q-2 specimen, as opposed to the CL-2 and D-2 specimens, is illustrated in Figure 10.

The relatively high crack growth rates of the Q specimens were also found to be affected by the stress ratio as illustrated in Figures 11 and 12. As the stress ratio was increased, the maximum stress intensity at a given crack length (say, a = 1.0 inch) approached the fracture toughness of the Q heat. It would, therefore, appear that the very high crack growth rates for the high stress ratios were due to Region III behavior, i.e., the specimens were on the verge of failure when the tests were begun.

The effect of varying the stress ratio on the crack growth rates of the CL and D specimens was not so obvious. Figure 13 presents the average crack growth rates of the CL and D specimens and the average crack growth rates from similar tests performed on similar martensitic steels(2). This comparison indicates that variations in stress ratio may have an effect upon the crack growth rates of steels possessing levels of fracture toughness similar to those of the CL and D specimens.

ClibPDF - www.fastio.com

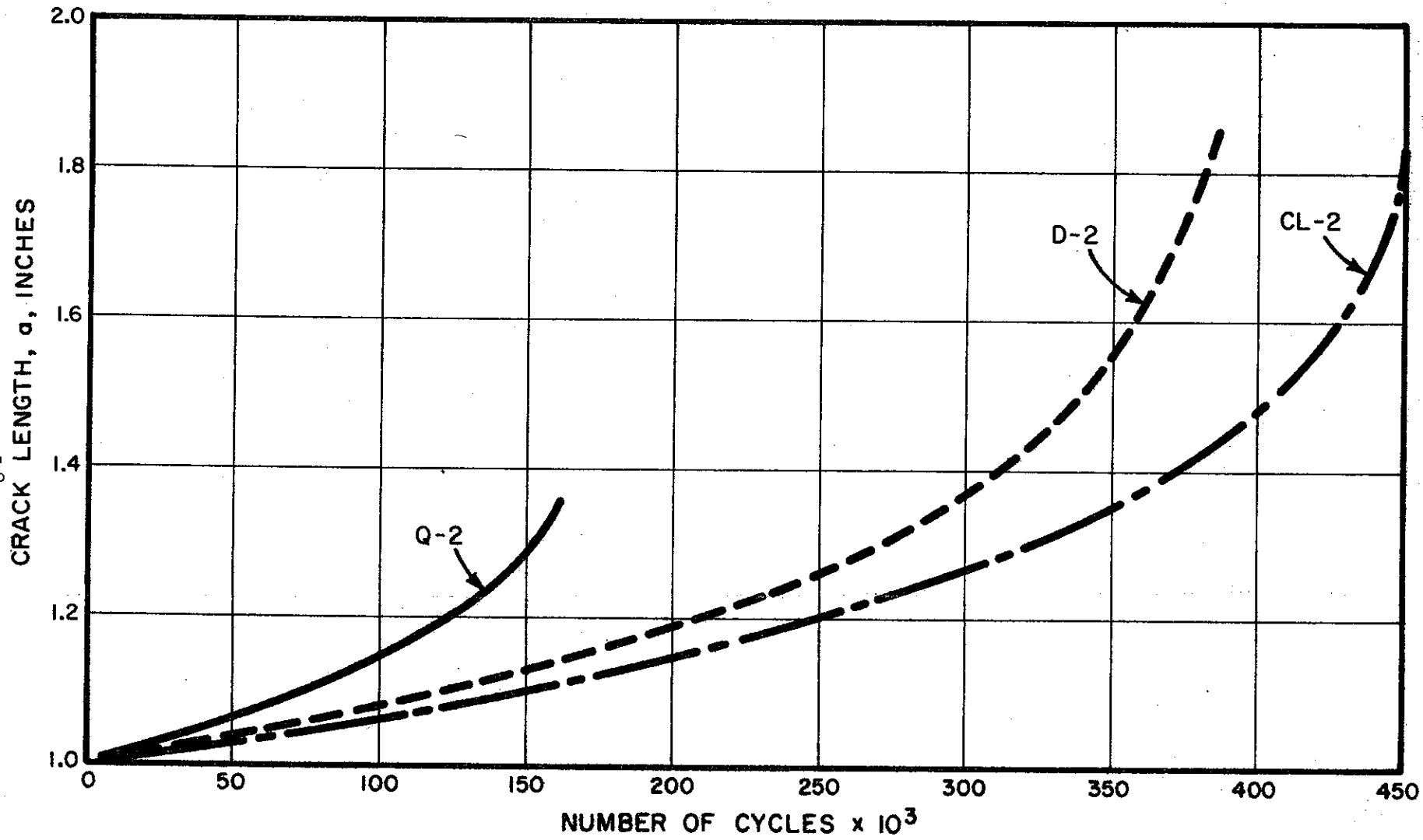

TYPICAL "a" VERSUS "N" CURVES
FOR VARIOUS HEATS, R = 0.73

FIGURE 8

ClibPDF - www.fastio.com

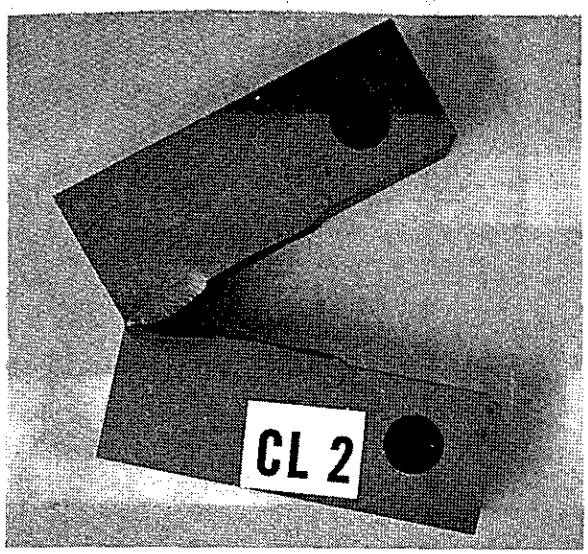

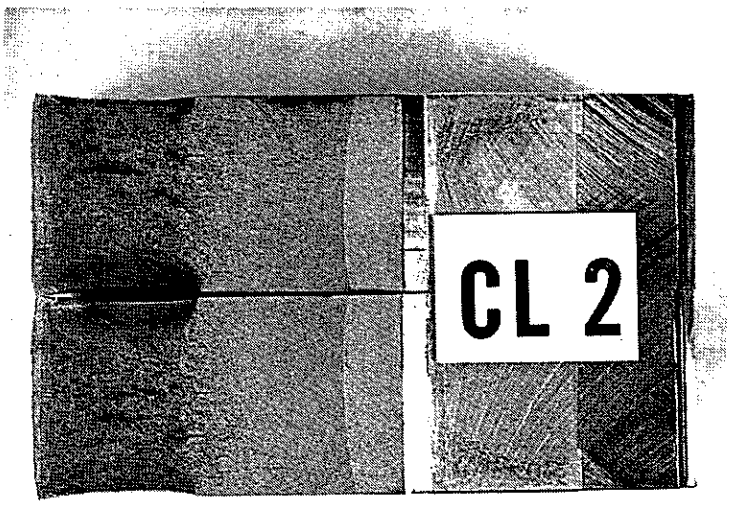

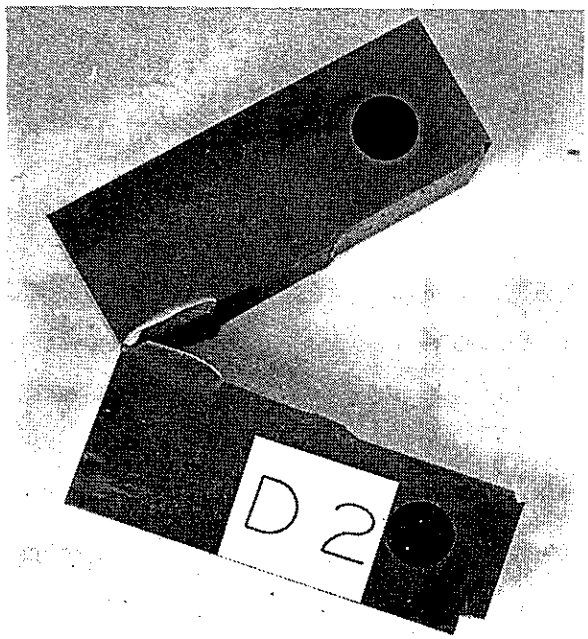

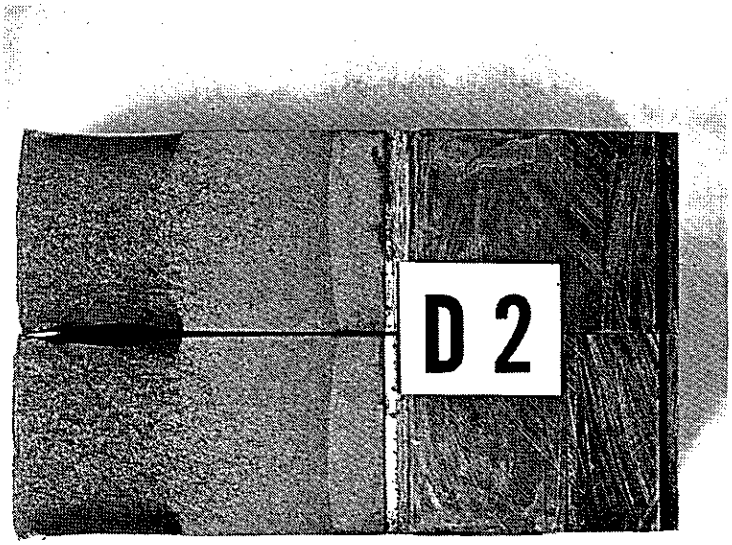

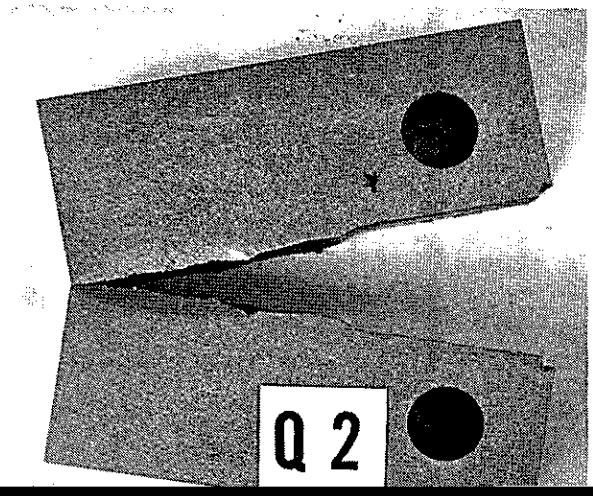

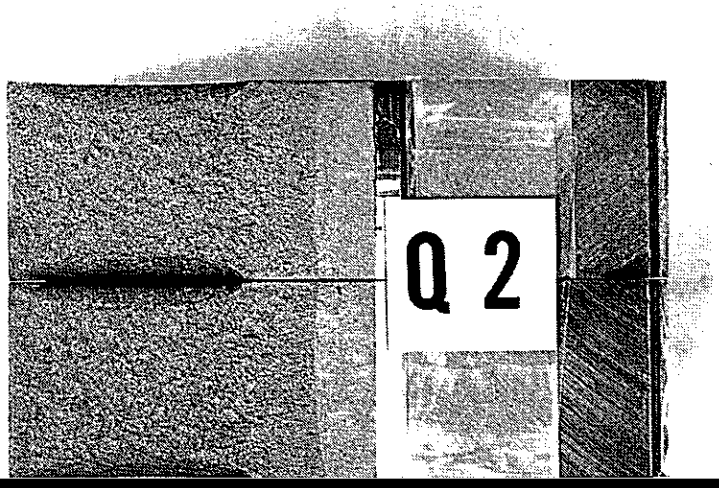

ClibPDF - www.fastio.com

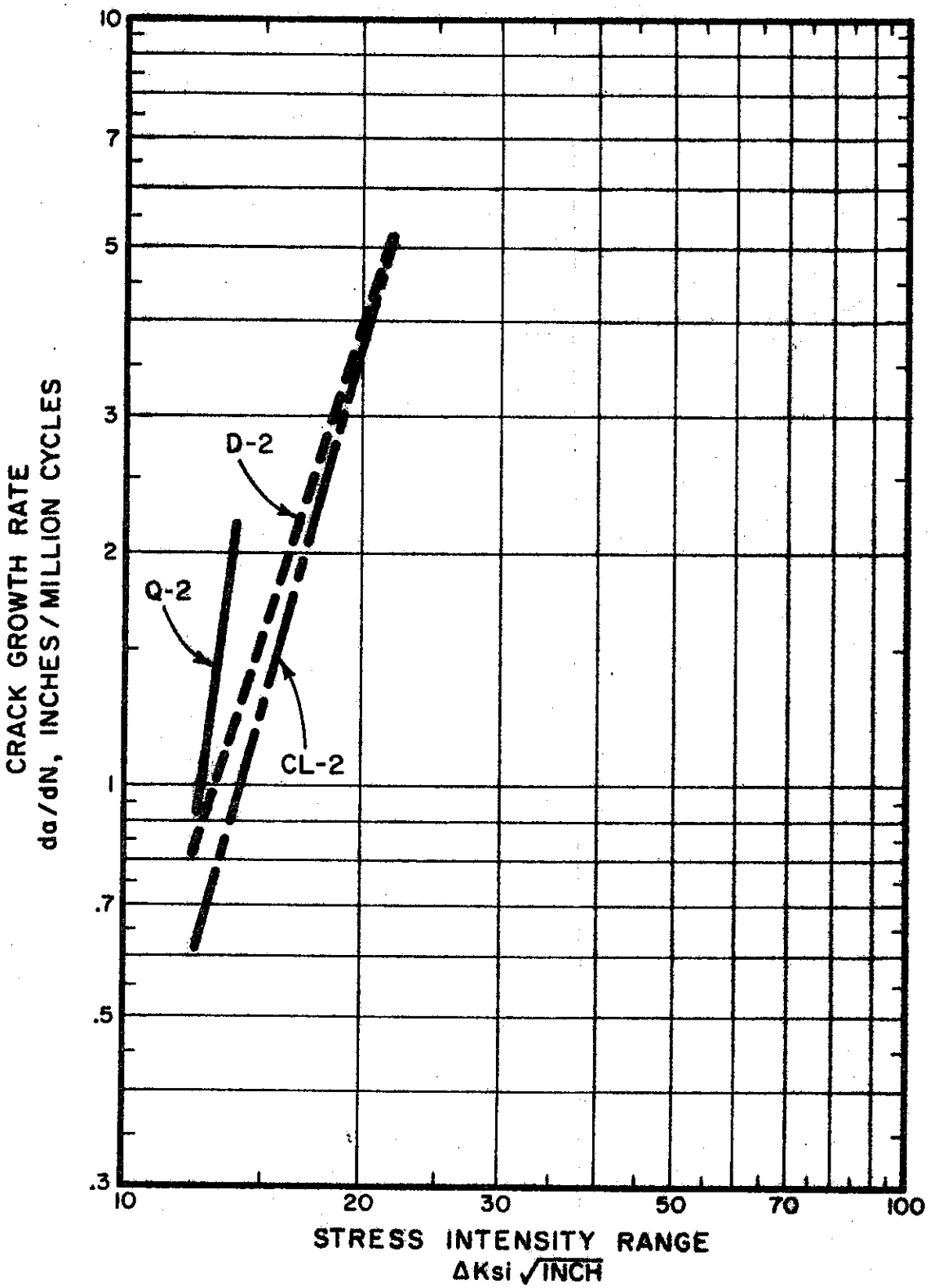

TYPICAL "da/dN" VERSUS "ΔK" CURVES
FOR VARIOUS HEATS, R=0.73

FIGURE 10

ClibPDF - www.fastio.com

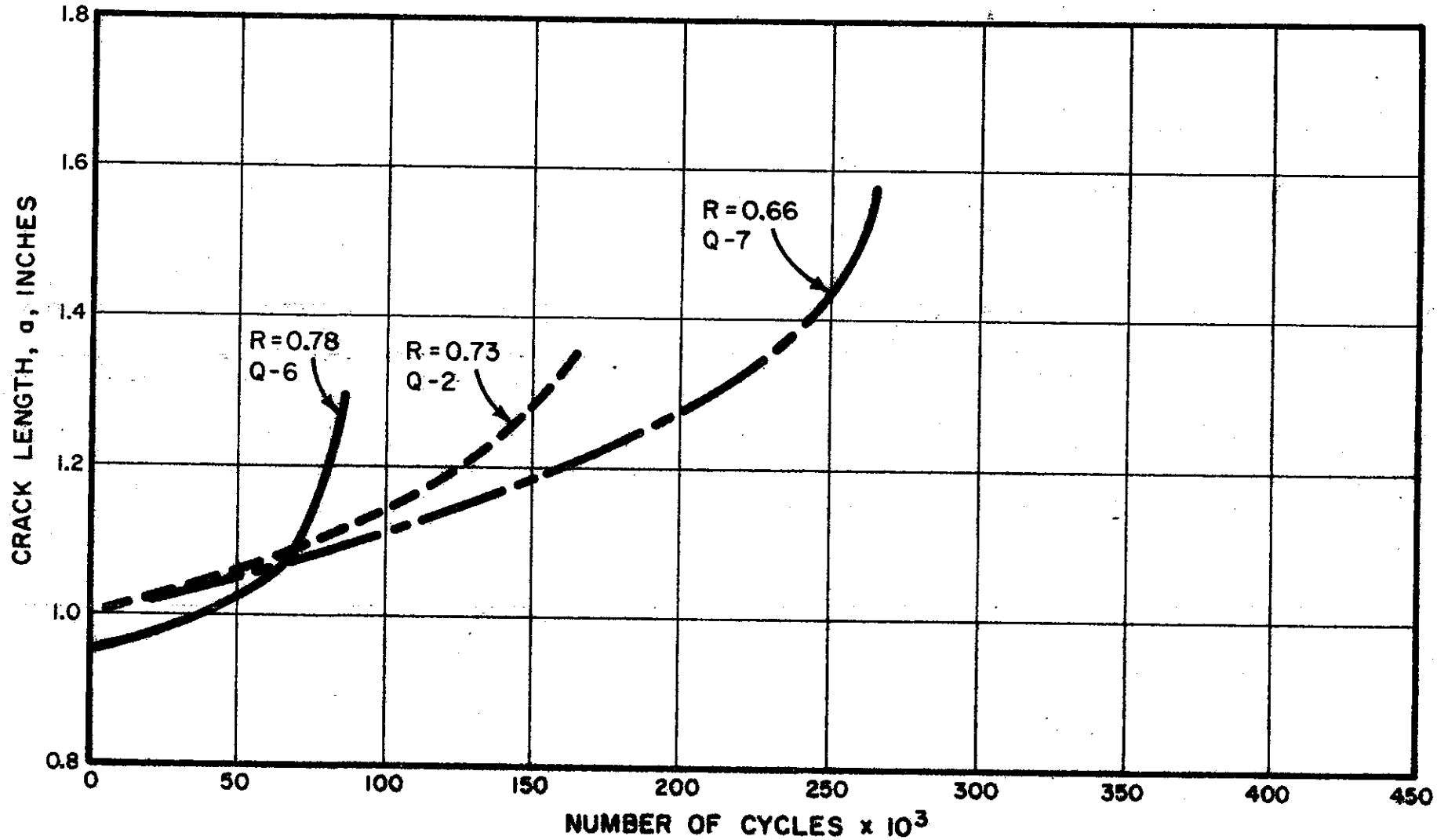

TYPICAL "a" VERSUS "N" CURVES
FOR VARIOUS STRESS RATIOS, HEAT Q

FIGURE 11

ClibPDF - www.fastio.com

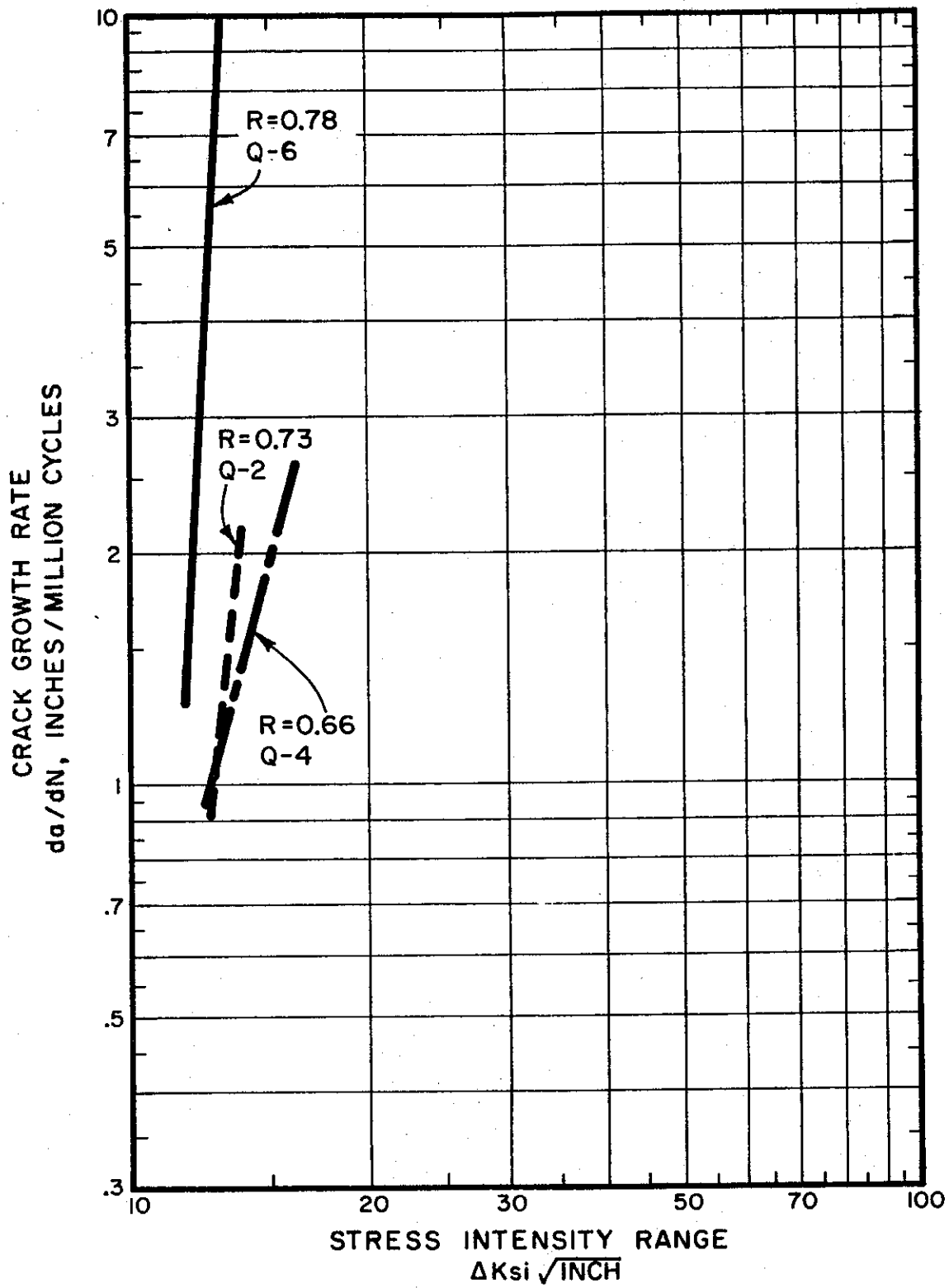

TYPICAL "da/dN" VERSUS "ΔK" CURVES
FOR VARIOUS STRESS RATIOS, HEAT Q

FIGURE 12

ClibPDF - www.fastio.com

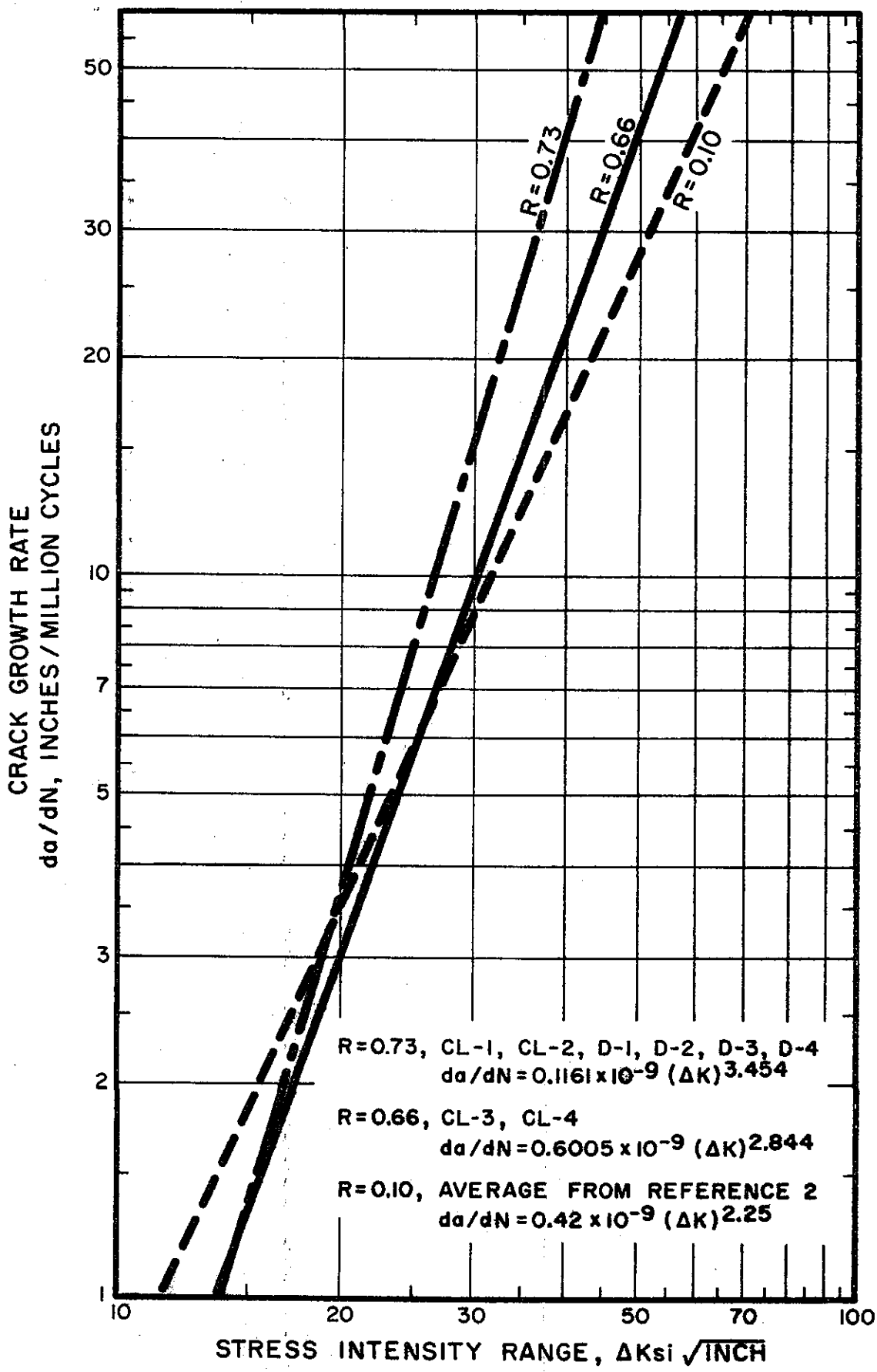

"da/dN" VERSUS "ΔK" CURVES FOR VARIOUS STRESS RATIOS, HEATS CL AND D

FIGURE 13

ClibPDF - www.fastio.com

V. REFERENCES

1. AASHTO Interim Specifications Bridges, 1974.

2. Barsom, J. M. and Novak, S. R., "Subcritical Crack Growth in Steel Bridge Members", Final Report NCHRP 12-14, September 1974.

3. Forman, R. G., Kerney, V. E. and Engle, "Numerical Analysis of Crack Propagation in Cyclic Loaded Structures", Journal of Basic Engineering, Paper No. 66-WA/Met-4 Trans. ASME Vol. 89, Series D, September 1967, p. 459.

4. "Fatigue Crack Growth Rate Laws Accounting for Stress-Ratio Effects" ASTM Task Force E24.04.04 Report No. 1, 1974.

5. Evans, P. R. V., Owen, N. B., McCantney, L. N., "Mean Stress Effect on Fatigue Crack Growth and Failure in Rail Steel", Engineering Fracture Mechanics, 1974, Vol. 6, pp 183-193.

6. Clark, W. G., Jr., Hudak, S. J., Jr., "Variability in Fatigue Crack Growth Rate Testing", An ASTM E-24.04.01 Task Group Report, Westinghouse Research Laboratories, September, 1974.

ClibPDF - www.fastio.com

V. APPENDIX

A. Test Results for Each Specimen

For each specimen the following figures present:

1. Fracture face photos;

2. Log-log plots of the "da/dN" versus "ΔK" data which appeared to be linear; and

3. The "best fit" equation for the crack growth rate.

ClibPDF - www.fastio.com

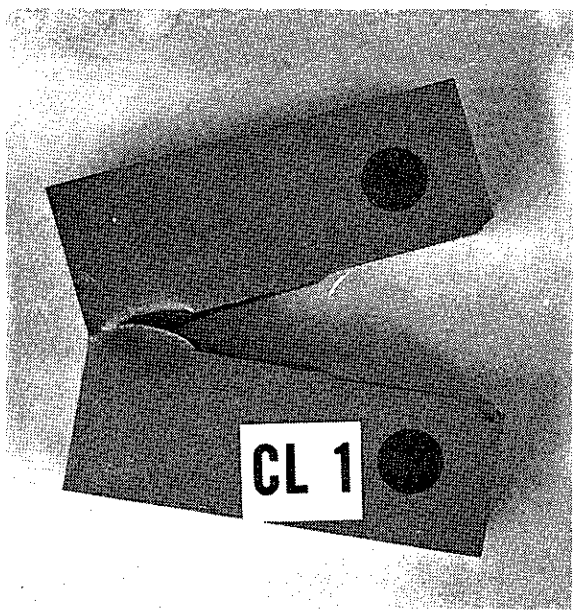

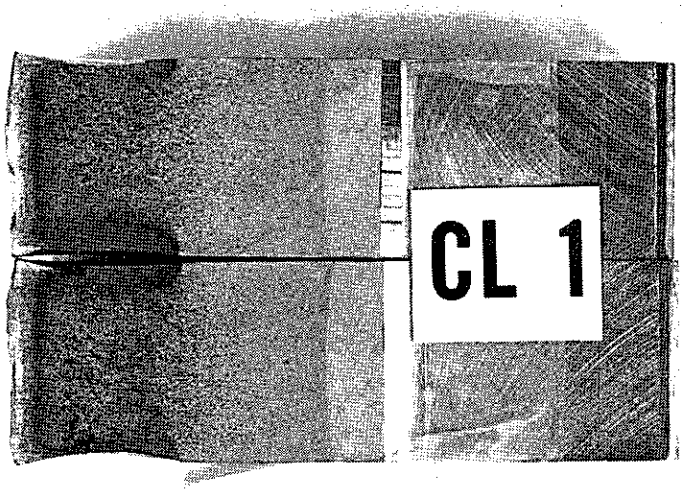

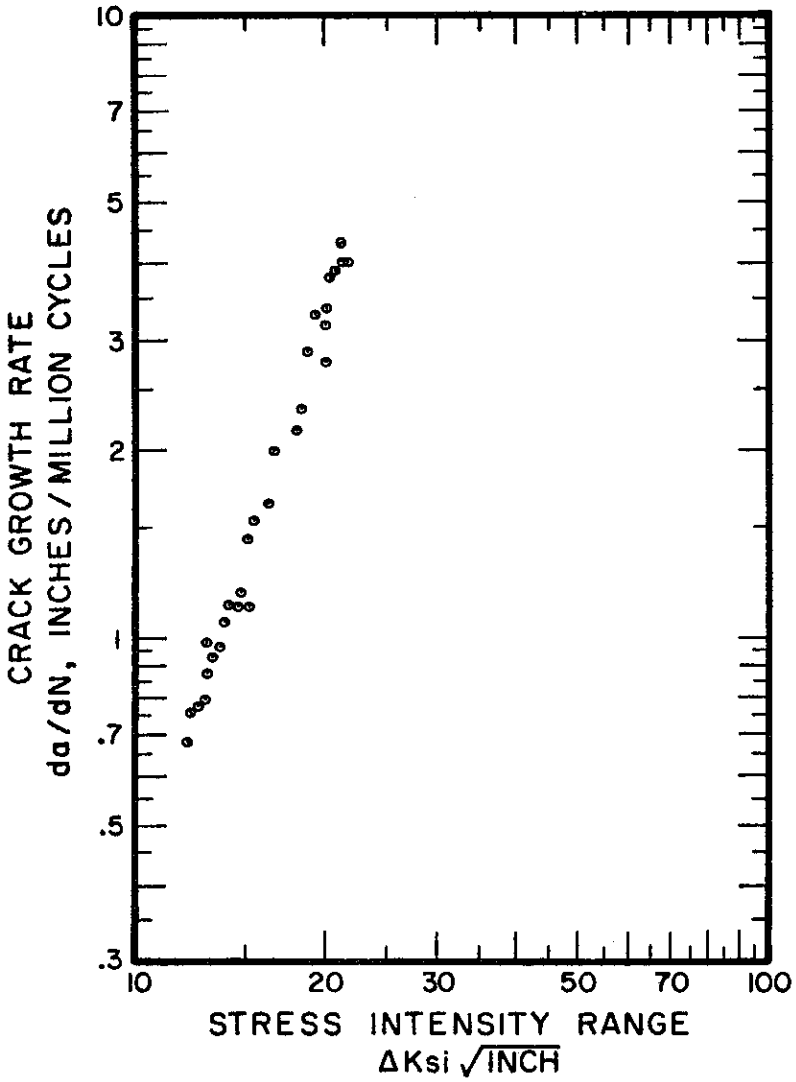

$R = 0.73$

$C = .2510 \times 10^{-9}$

$M = 3.150$

$\frac{da}{dN} = C(\Delta K)^M$

SPECIMEN CL-I TEST RESULTS

FIGURE AI

ClibPDF - www.fastio.com

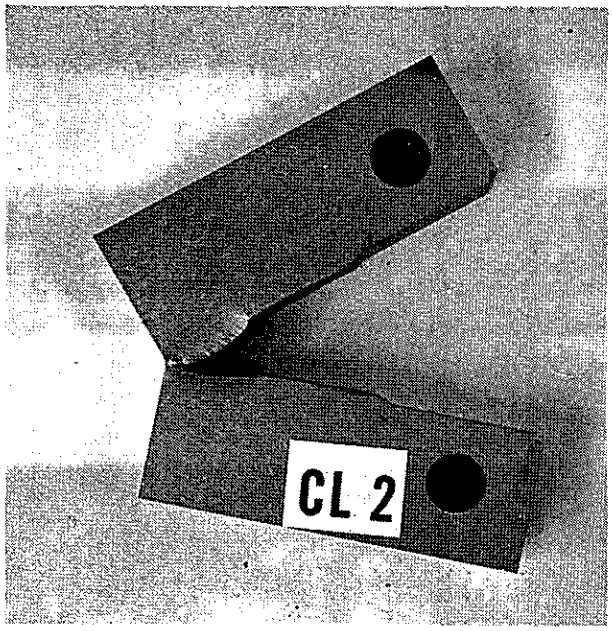

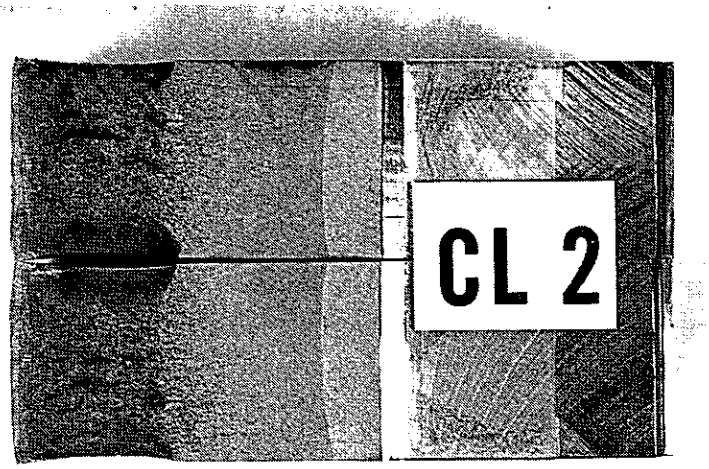

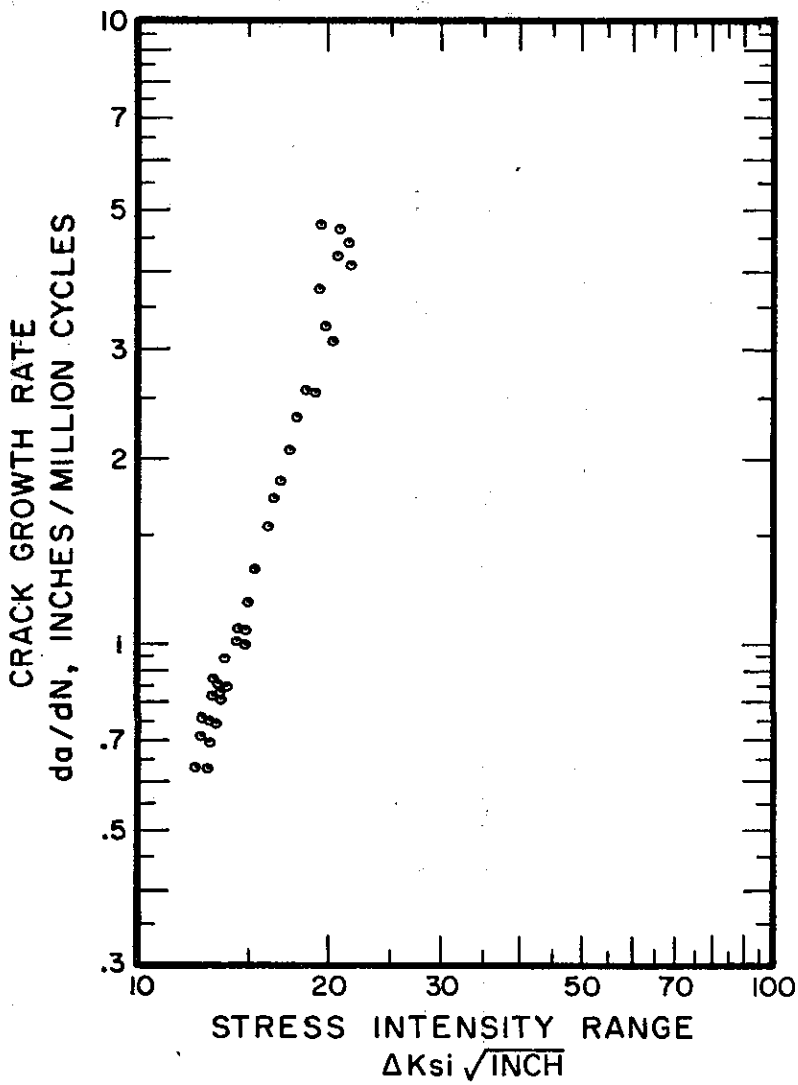

$R = 0.73$

$C = .6560 \times 10^{-10}$

$M = 3.641$

$$\frac{da}{dN} = C(\Delta K)^M$$

SPECIMEN CL-2 TEST RESULTS

FIGURE A2

ClibPDF - www.fastio.com

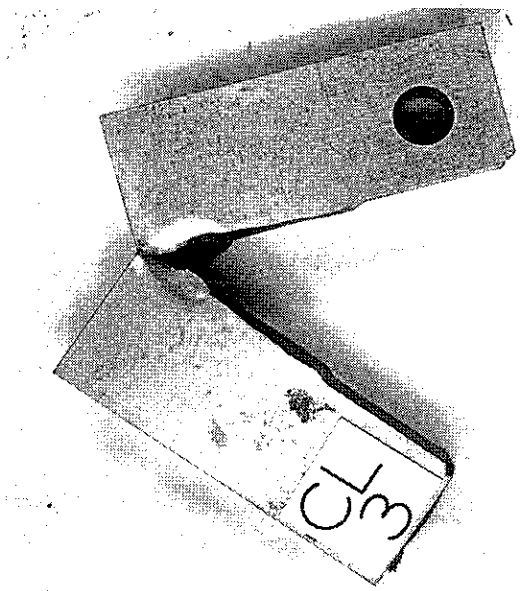

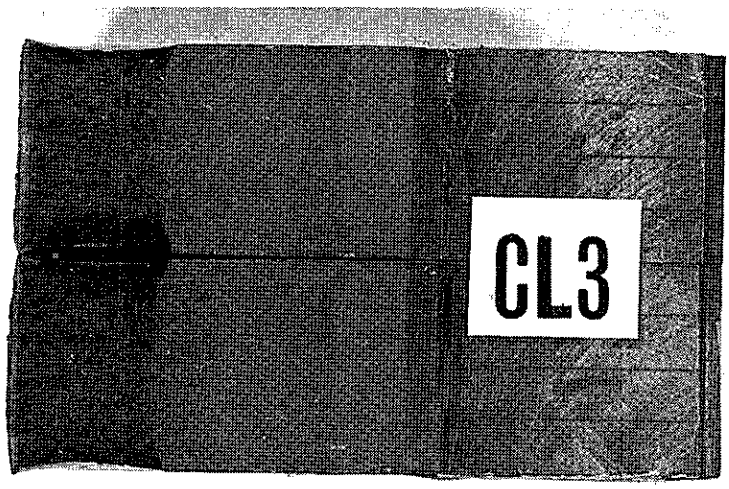

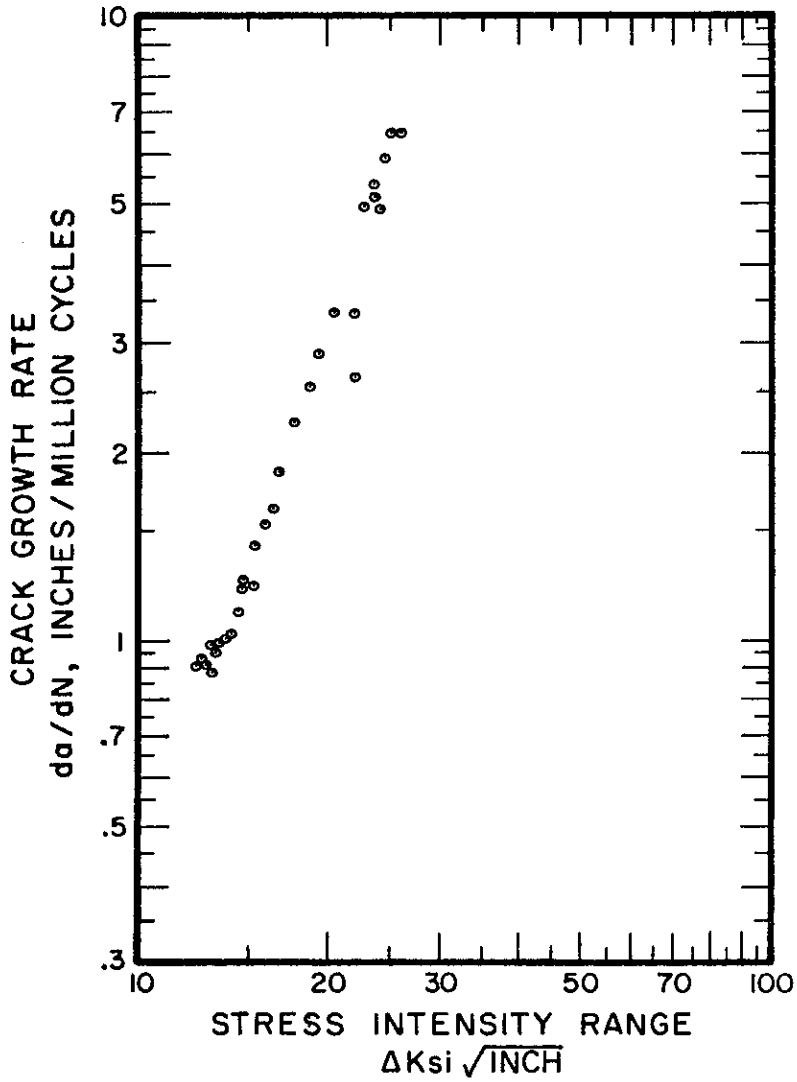

$R = 0.66$

$C = .7579 \times 10^{-9}$

$M = 2.761$

$$\frac{da}{dN} = C(\Delta K)^M$$

SPECIMEN CL-3 TEST RESULTS

FIGURE A3

ClibPDF - www.fastio.com

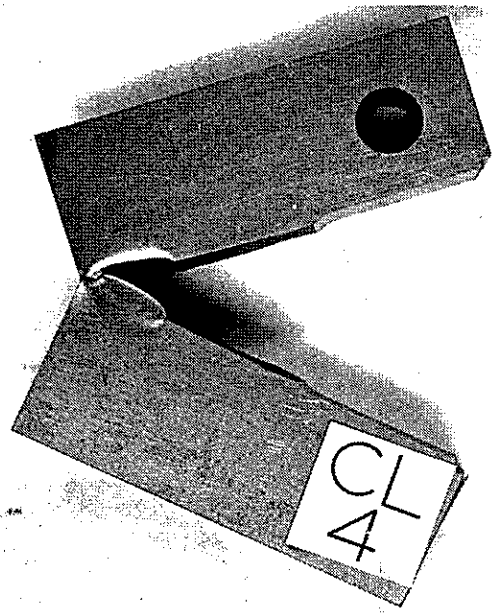

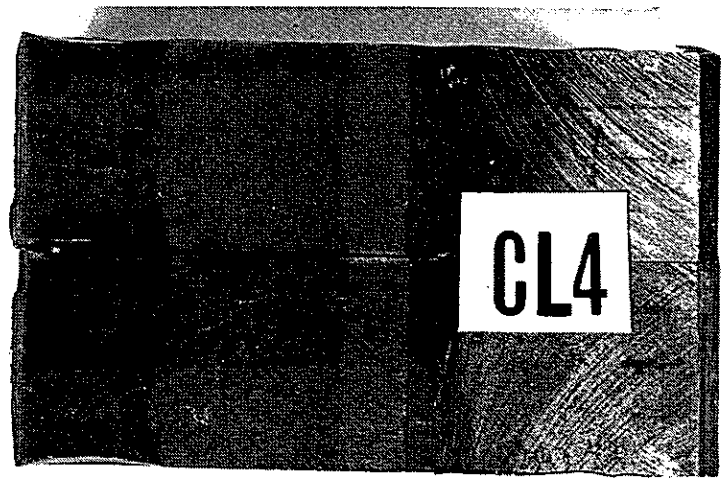

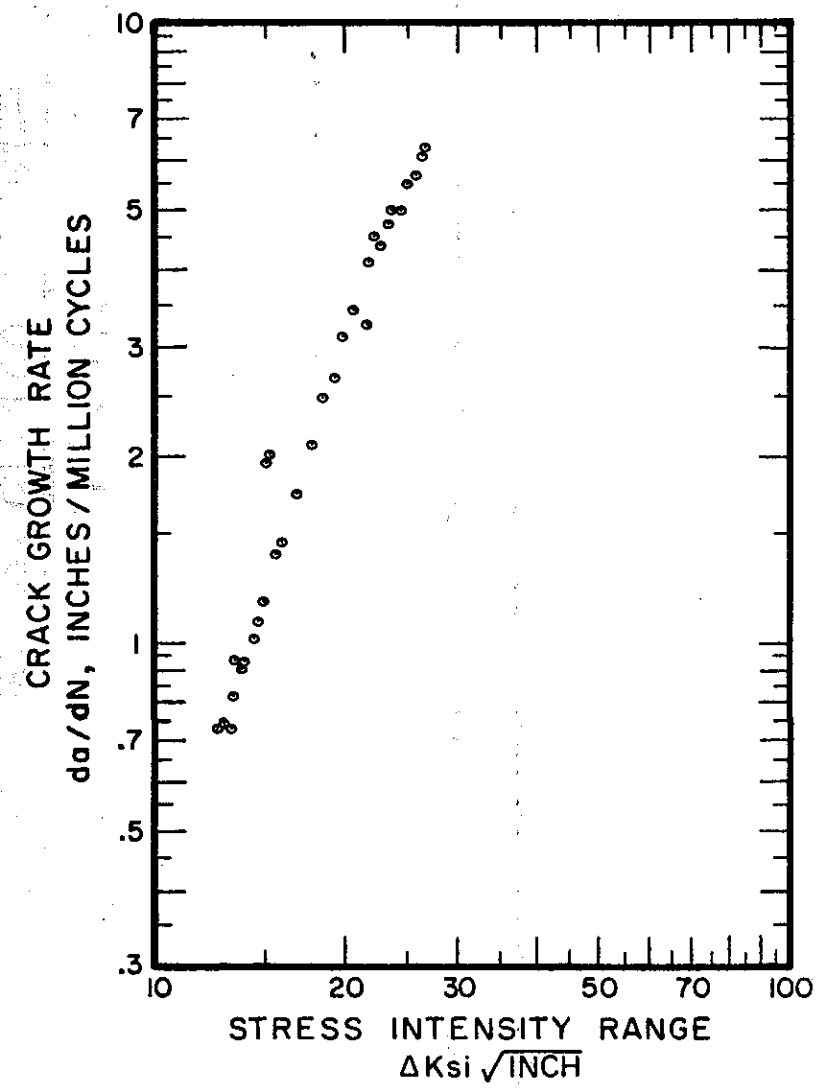

$R = 0.66$

$C = .4757 \times 10^{-9}$

$M = 2.927$

$$\frac{da}{dN} = C(\Delta K)^M$$

SPECIMEN CL-4 TEST RESULTS

FIGURE A4

ClibPDF - www.fastio.com

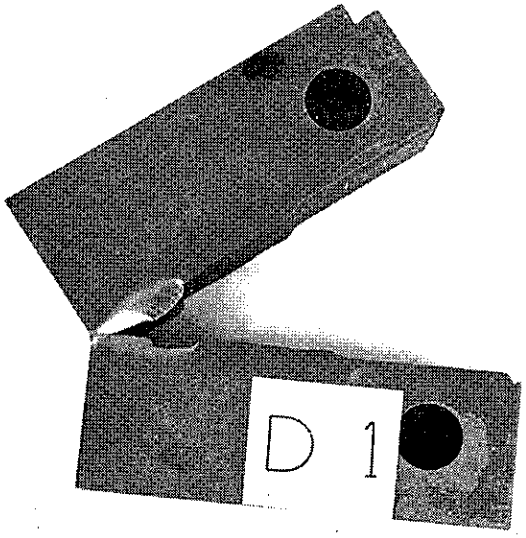

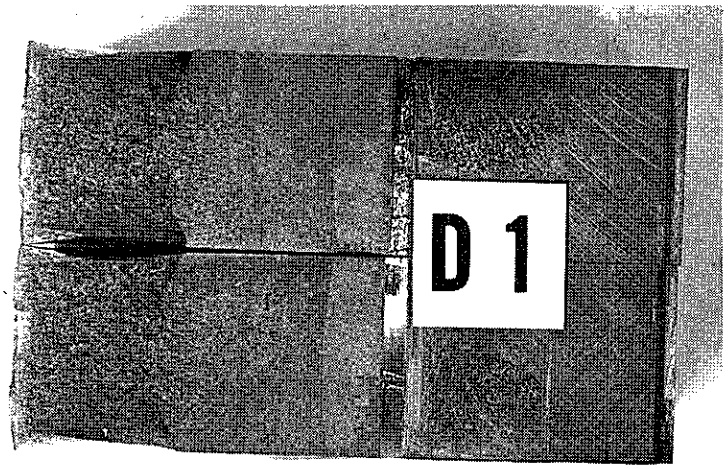

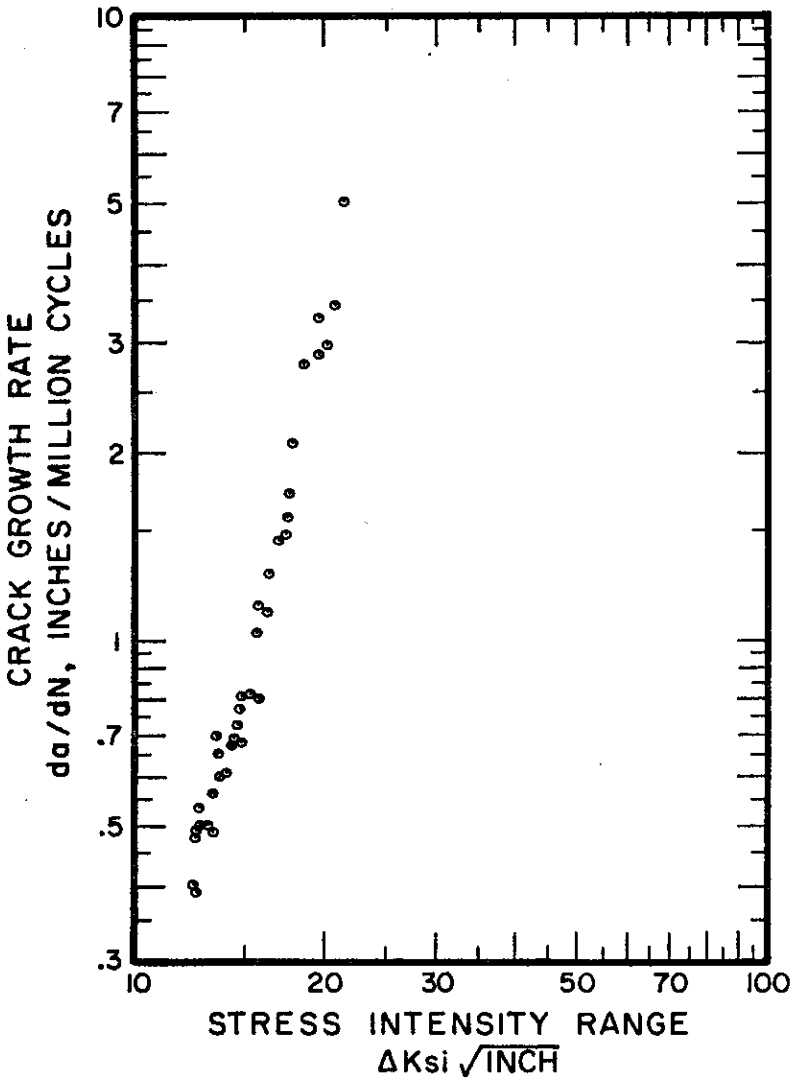

$R = 0.73$

$C = .1051 \times 10^{-10}$

$M = 4.200$

$$\frac{da}{dN} = C(\Delta K)^M$$

SPECIMEN D-I TEST RESULTS

FIGURE A5

ClibPDF - www.fastio.com

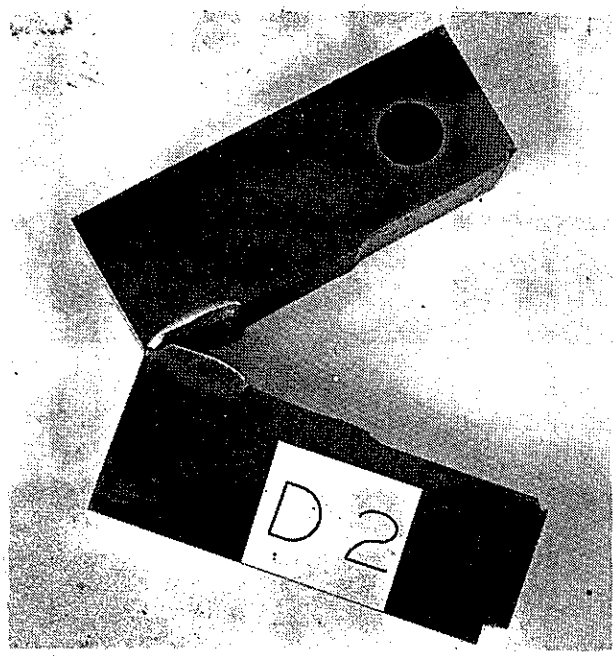

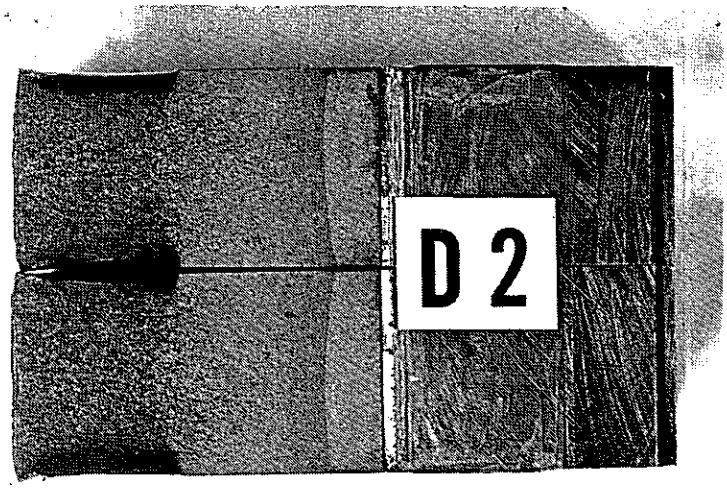

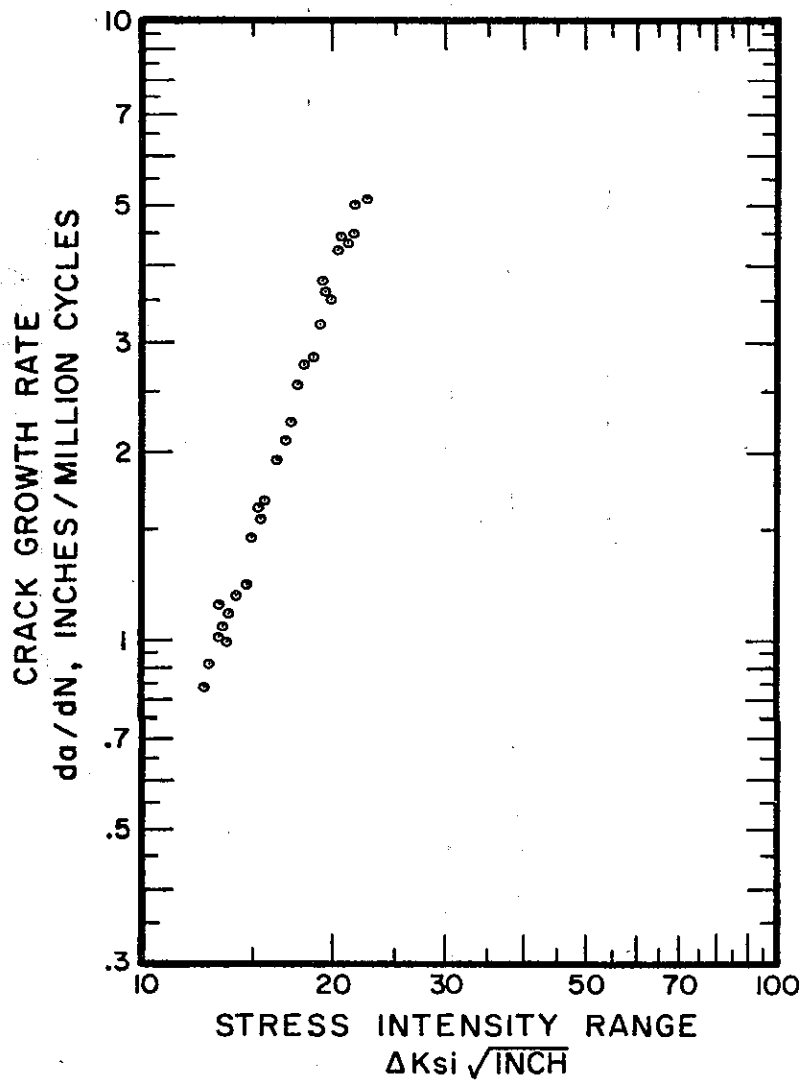

$R = 0.73$

$C = .2512 \times 10^{-9}$

$M = 3.219$

$$\frac{da}{dN} = C(\Delta K)^M$$

SPECIMEN D-2 TEST RESULTS

FIGURE A6

ClibPDF - www.fastio.com

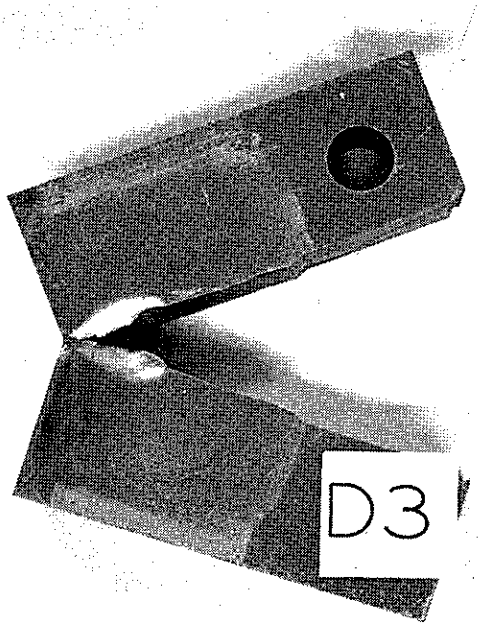

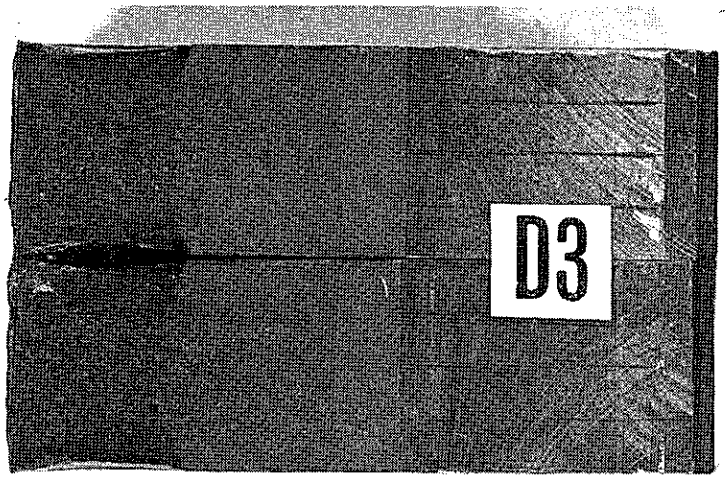

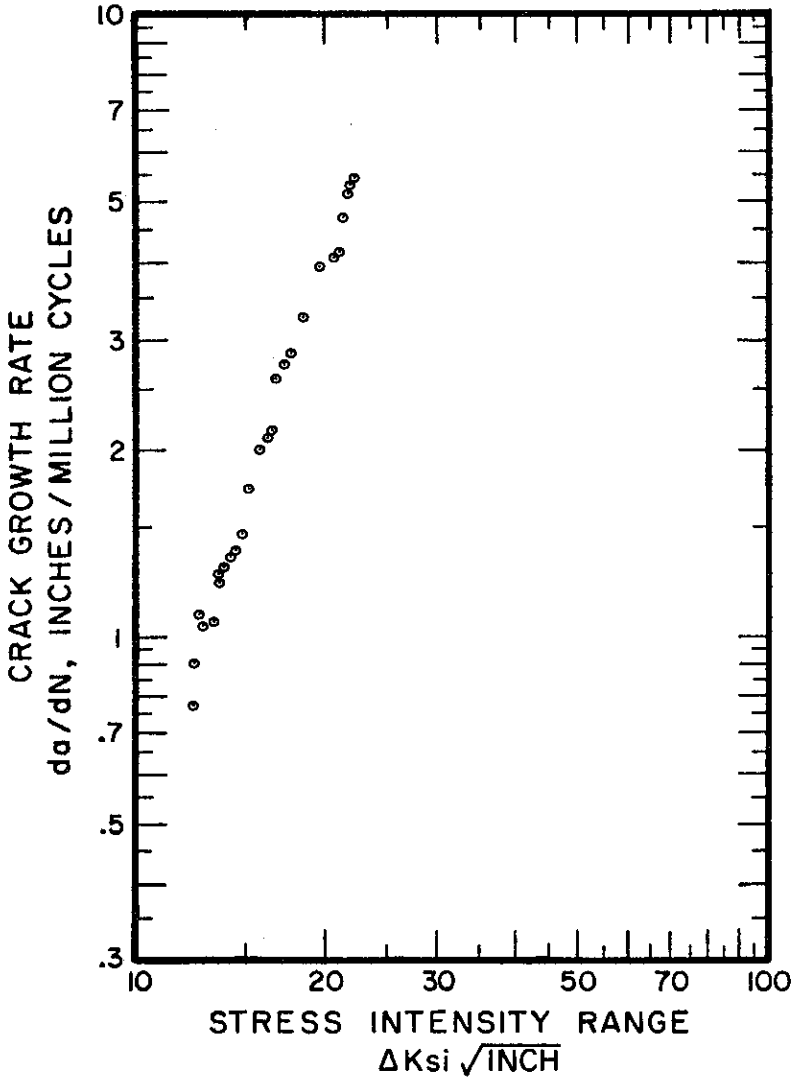

$R = 0.73$

$C = .3525 \times 10^{-9}$

$M = 3.114$

$$\frac{da}{dN} = C(\Delta K)^M$$

SPECIMEN D-3 TEST RESULTS

FIGURE A7

ClibPDF - www.fastio.com

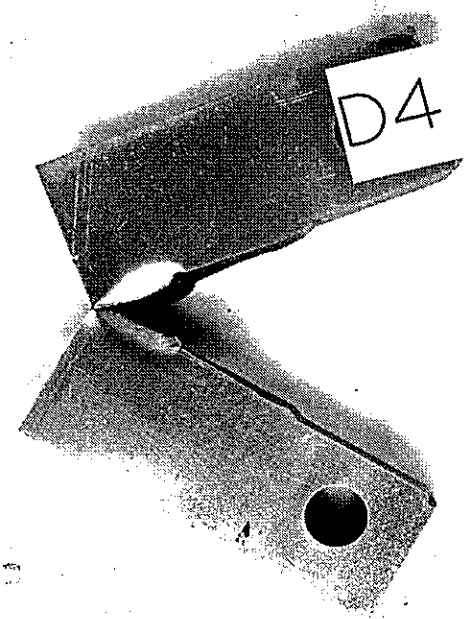

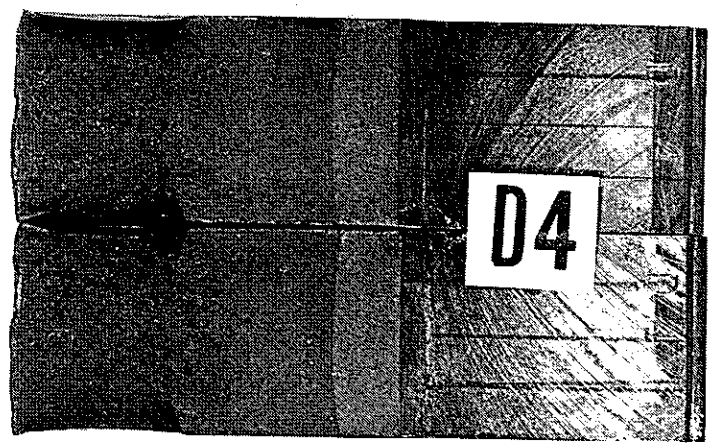

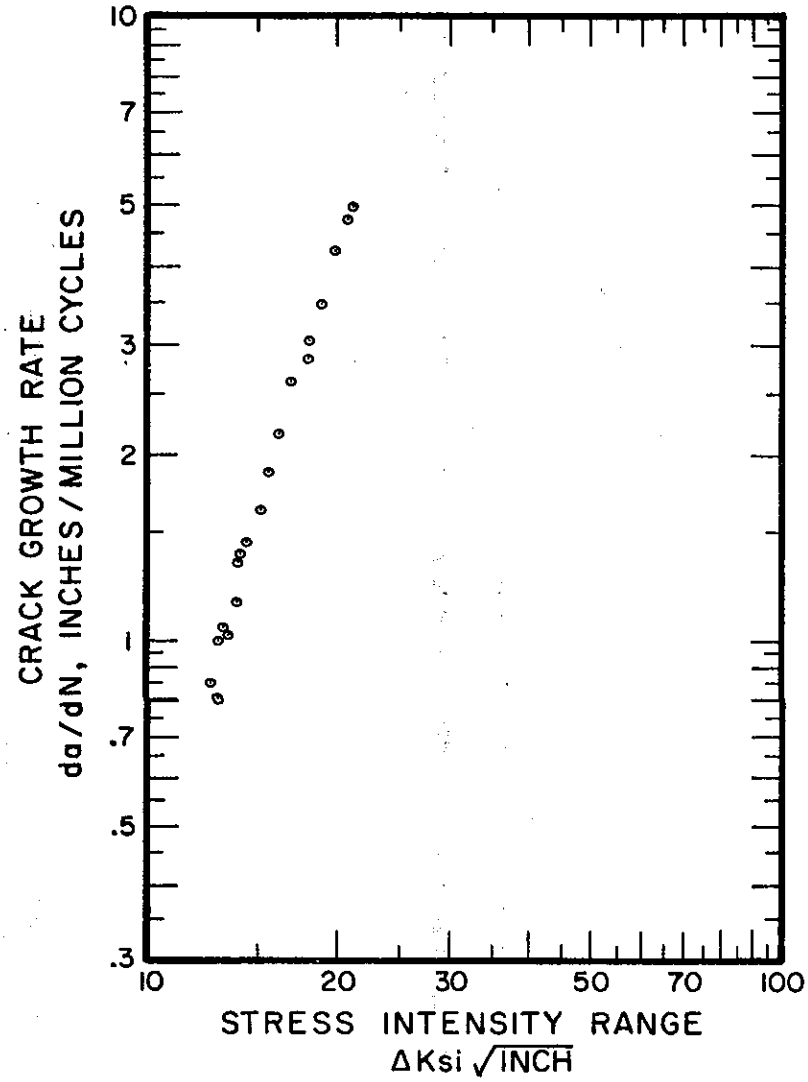

$R = 0.73$

$C = .1602 \times 10^{-9}$

$M = 3.401$

$$\frac{da}{dN} = C(\Delta K)^M$$

SPECIMEN D-4 TEST RESULTS

FIGURE A8

ClibPDF - www.fastio.com

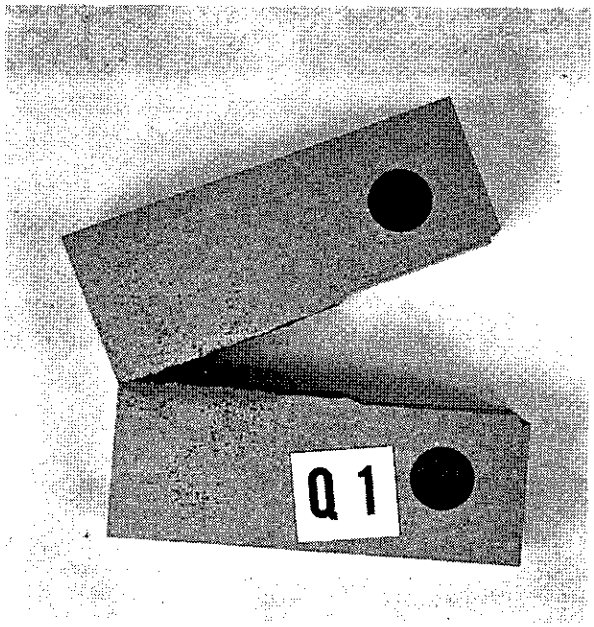

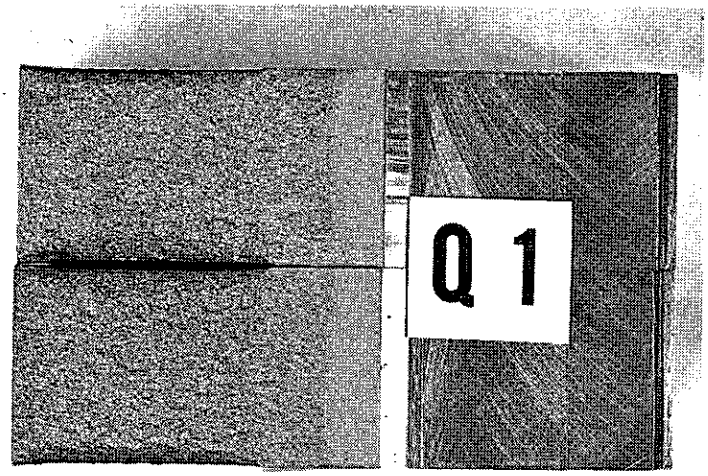

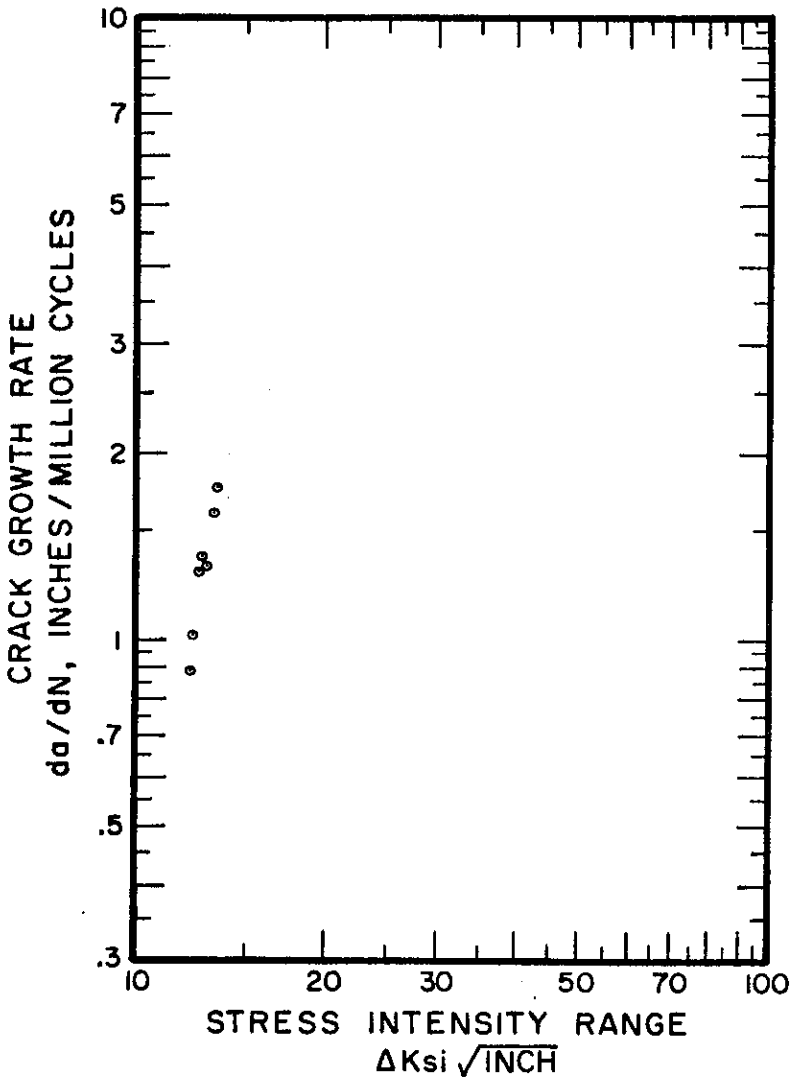

$R = 0.73$

$C = .2656 \times 10^{-12}$

$M = 6.030$

$$\frac{da}{dN} = C(\Delta K)^M$$

SPECIMEN Q-1 TEST RESULTS

FIGURE A9

ClibPDF - www.fastio.com

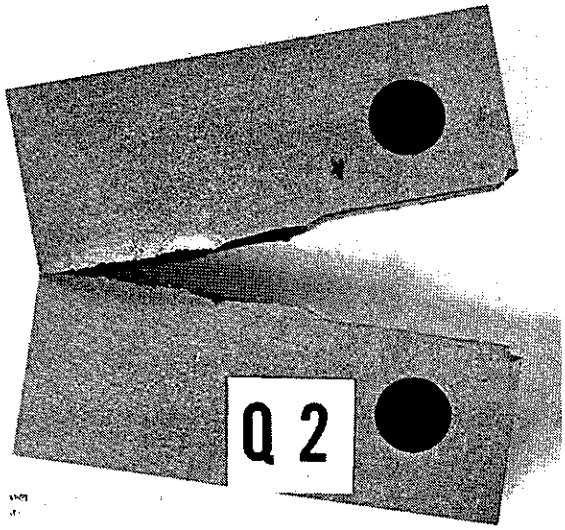

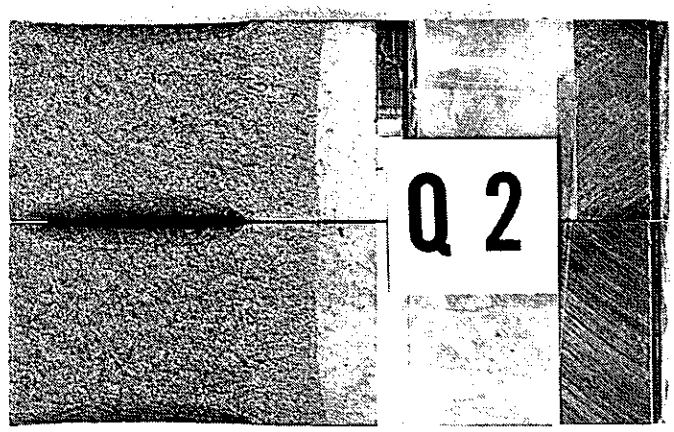

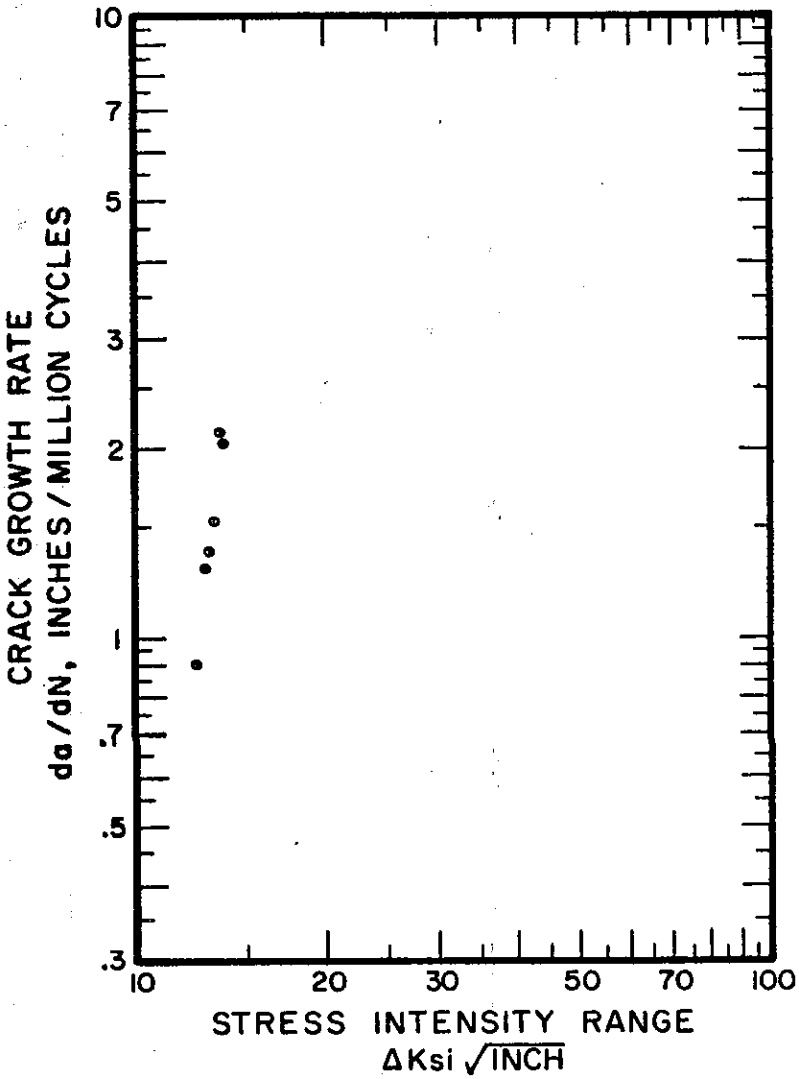

$R = 0.73$

$C = .3228 \times 10^{-15}$

$M = 8.620$

$$\frac{da}{dN} = C(\Delta K)^M$$

SPECIMEN Q-2 TEST RESULTS

FIGURE A10

ClibPDF - www.fastio.com

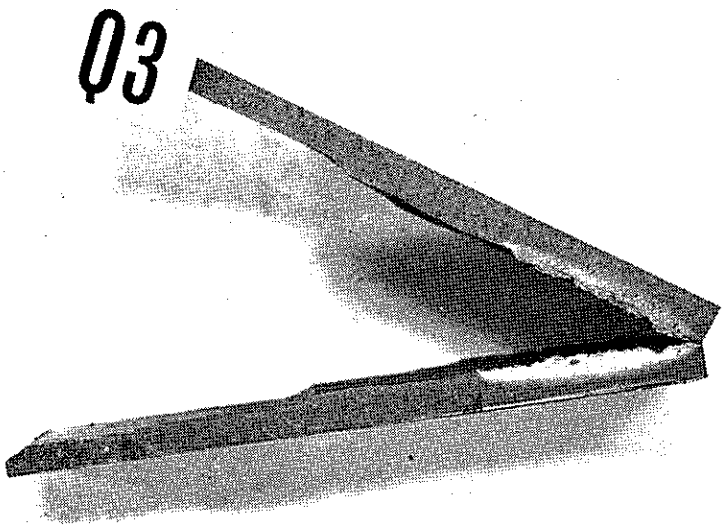

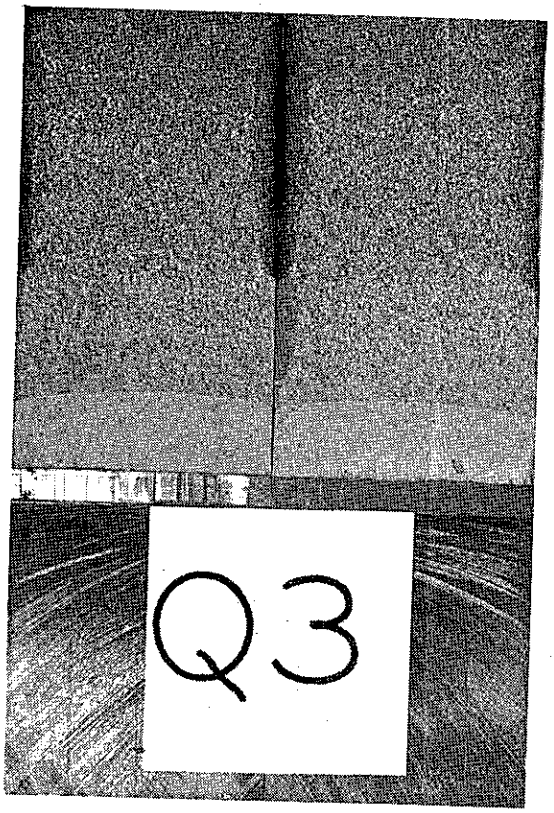

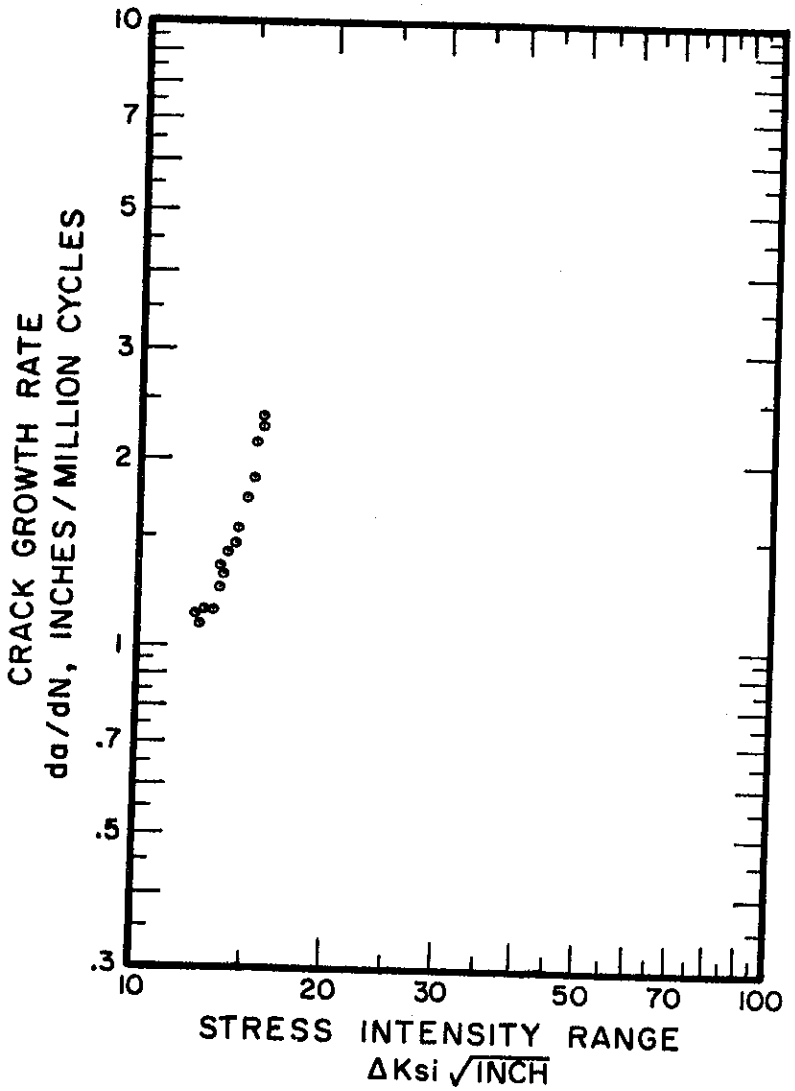

NOTE:
OUTER PORTIONS OF SPECIMEN REMOVED AFTER COMPACT TENSION TEST

$R = 0.66$

$C = .2385 \times 10^{-9}$

$M = 3.307$

$$\frac{da}{dN} = C(\Delta K)^M$$

SPECIMEN Q-3 TEST RESULTS

FIGURE A11

ClibPDF - www.fastio.com

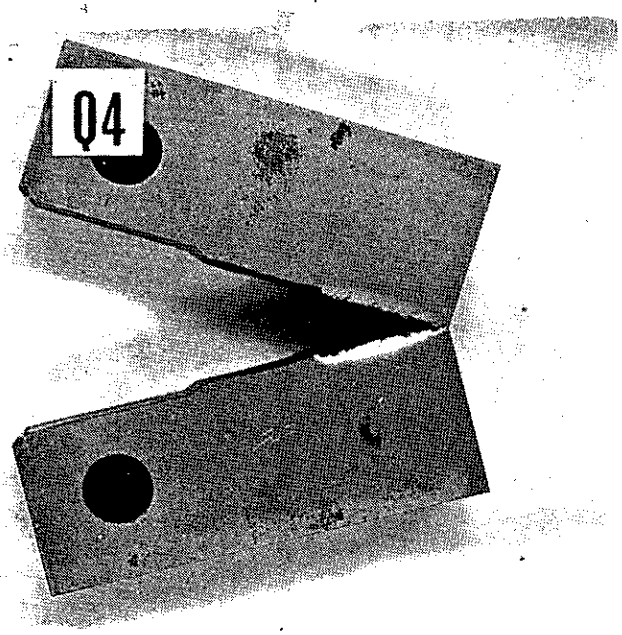

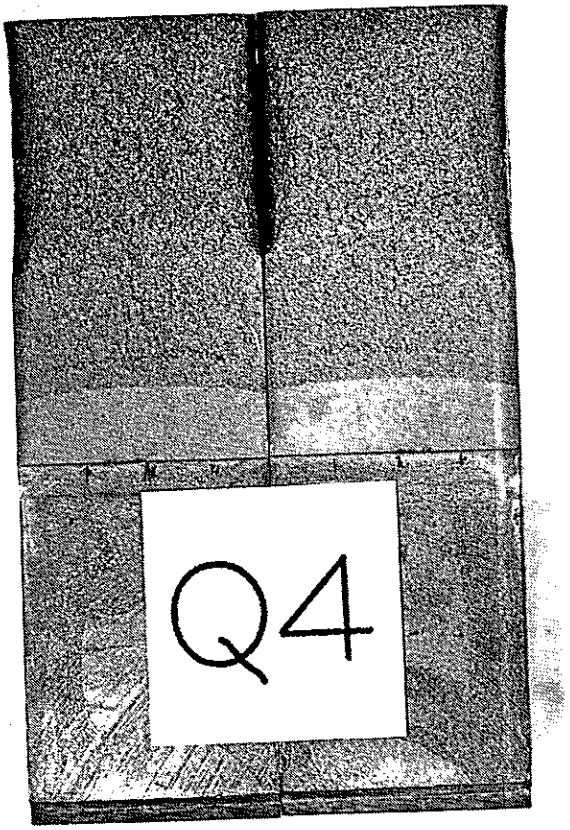

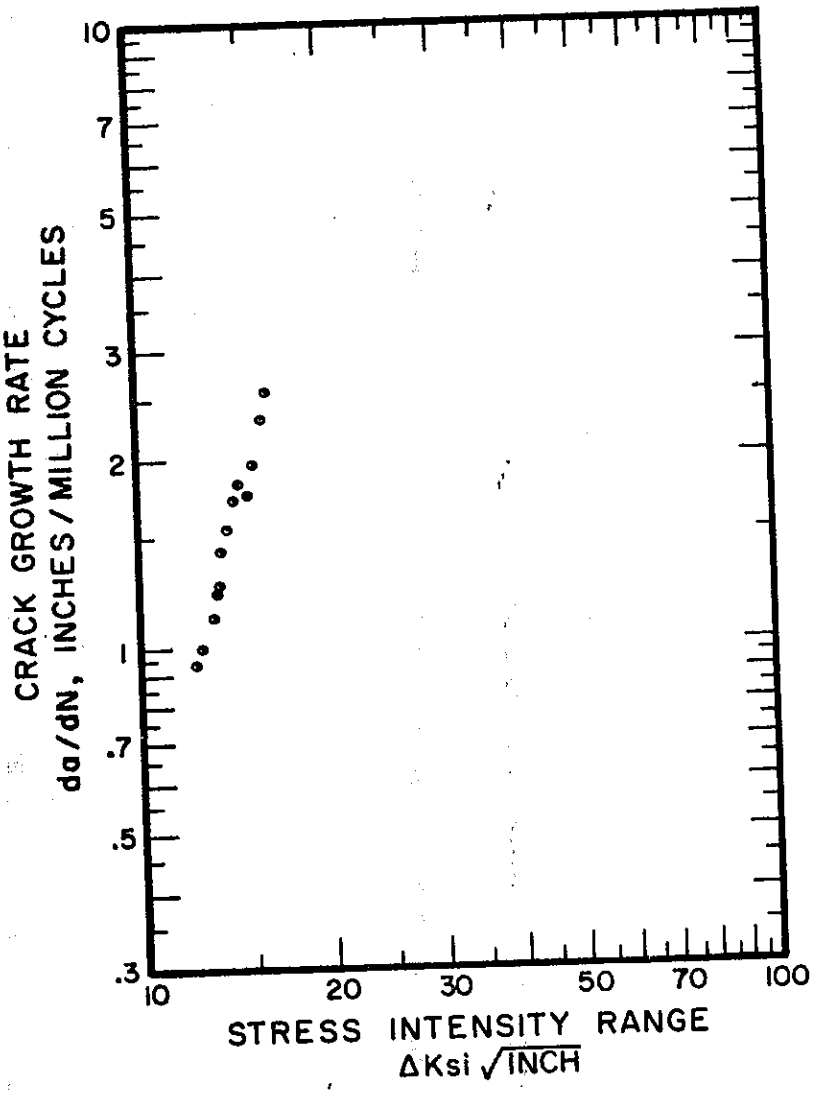

$R = 0.66$

$C = .8531 \times 10^{-10}$

$M = 3.702$

$\frac{da}{dN} = C(\Delta K)^M$

SPECIMEN Q-4 TEST RESULTS

FIGURE A12

ClibPDF - www.fastio.com

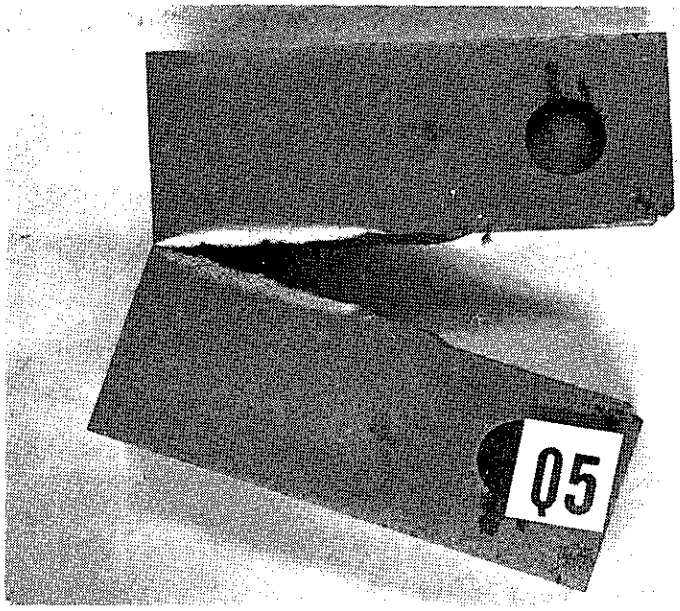

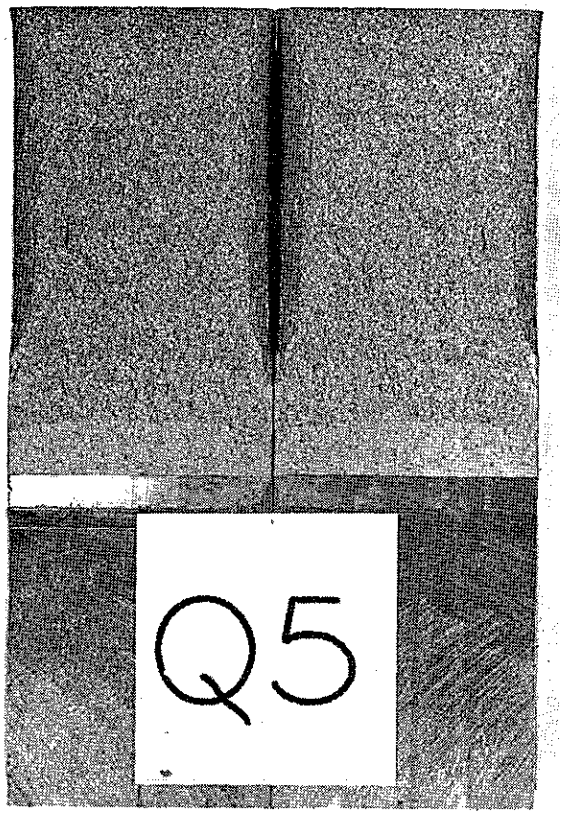

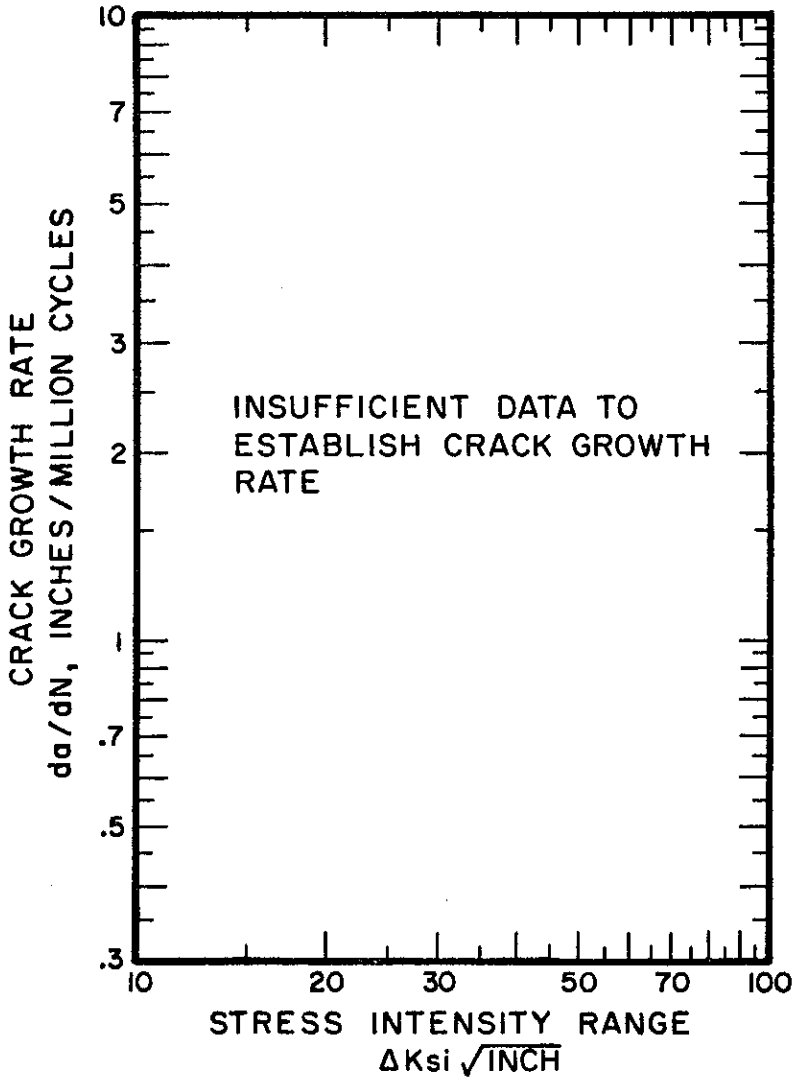

R = 0.78

C =

M =

$$\frac{da}{dN} = C(\Delta K)^M$$

SPECIMEN Q-5 TEST RESULTS

FIGURE A13

ClibPDF - www.fastio.com

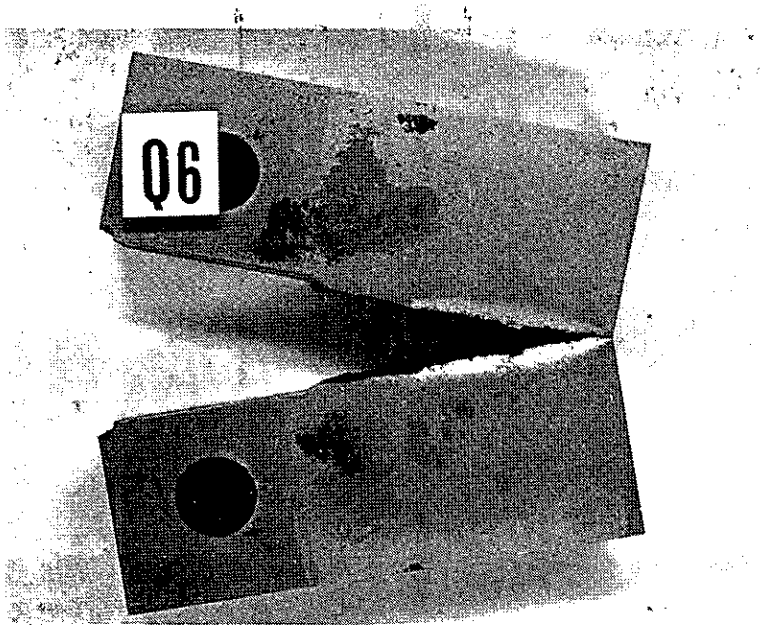

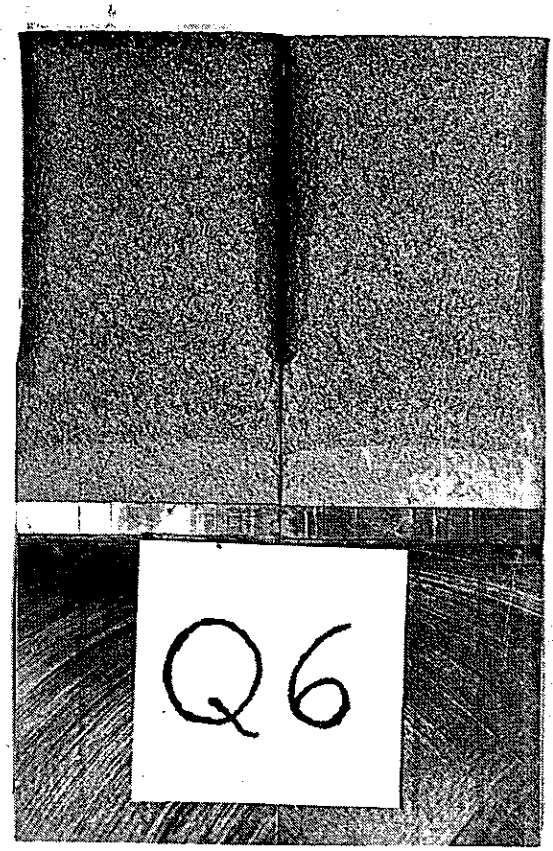

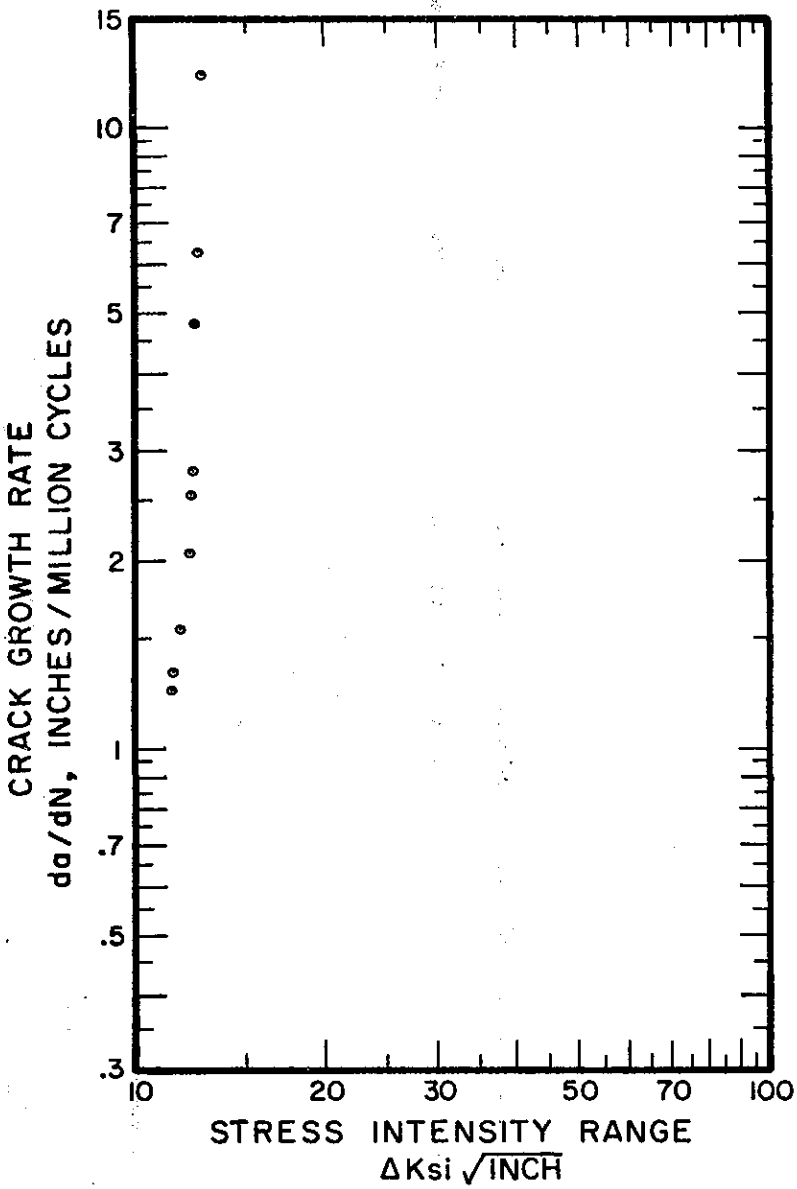

$R = 0.78$

$C = .7346 \times 10^{-24}$

$M = 17.08$

$$\frac{da}{dN} = C(\Delta K)^M$$

SPECIMEN Q-6 TEST RESULTS

FIGURE A14

ClibPDF - www.fastio.com

ClibPDF - www.fastio.com

ClibPDF - www.fastio.com